Werk

Jahr: 1988
Kollektion: fid.geo
Signatur: 8 Z NAT 2148:62
Digitalisiert: Niedersächsische Staats- und Universitätsbibliothek Göttingen
Werk Id: PPN1015067948_0062
PURL: http://resolver.sub.uni-goettingen.de/purl?PPN1015067948_0062

LOG Id: LOG_0011
LOG Titel: Near-vertical and wide-angle seismic surveys in the Black Forest, SW Germany
LOG Typ: article

Übergeordnetes Werk

Werk Id: PPN1015067948
PURL: http://resolver.sub.uni-goettingen.de/purl?PPN1015067948
OPAC: http://opac.sub.uni-goettingen.de/DB=1/PPN?PPN=1015067948

Contact

Niedersächsische Staats- und Universitätsbibliothek Göttingen
Georg-August-Universität Göttingen
Platz der Göttinger Sieben 1
37073 Göttingen
Germany
Email: gdz@sub.uni-goettingen.de

J Geophys (1987) 62:1–30

Journal of Geophysics

Original investigations

Near-vertical and wide-angle seismic surveys in the Black Forest, SW Germany

E. Lüschen [1], F. Wenzel [1], K.-J. Sandmeier [1], D. Menges [1], Th. Rühl [1], M. Stiller [2], W. Janoth [2], F. Keller [2], W. Söllner [2], R. Thomas [2], A. Krohe [3], R. Stenger [4], K. Fuchs [1], H. Wilhelm [1], and G. Eisbacher [3]

[1] Geophysikalisches Institut, Universität Karlsruhe, Hertzstrasse 16, D-7500 Karlsruhe 21, Federal Republic of Germany
[2] Institut für Geophysik, Technische Universität Clausthal, Arnold-Sommerfeld-Strasse 1, D-3392 Clausthal-Zellerfeld, Federal Republic of Germany
[3] Geologisches Institut, Universität Karlsruhe, Kaiserstrasse 12, D-7500 Karlsruhe, Federal Republic of Germany
[4] Mineralogisch-petrographisches Institut, Universität Freiburg, Albertstrasse 23b, D-7800 Freiburg, Federal Republic of Germany

Abstract. A unified seismic exploration program, consisting of 345 km of deep reflection profiling, a 240-km refraction profile, an expanding-spread profile and near-surface high-resolution measurements, revealed a strongly differentiated crust beneath the Black Forest. The highly reflective lower crust contains numerous horizontal and dipping reflectors at depths of 13–14 km down to the crust-mantle boundary (Moho). The Moho appears as a flat and horizontal first-order discontinuity at a relatively shallow level of 25–27 km above a transparent upper mantle. In the seismic model based on near-vertical and wide-angle data, the lower crust consists of lamellae with an average thickness of about 100 m and velocity contrasts increasing with depth. The upper crust is characterized by a discontinuous pattern of mostly dipping reflectors which are related to Hercynian overthrusting and accretion and to late-Hercynian extensional faulting. A bright spot at 9.5 km depth is interpreted to be due to low-velocity material. The lower part of the upper crust appears as a relatively transparent zone which is also identified as a low-velocity zone situated directly above the laminated lower crust.

Key words: Reflection seismology – Deep-crustal reflection profiling – Refraction seismology – Hercynian crustal evolution

1 Introduction

Continental deep drilling is one of the key projects of the International Lithosphere Program (ILP) which is aimed at unravelling the dynamics and evolution of the lithosphere. The contribution of the Federal Republic of Germany consists of the continental deep-drilling program, KTB (Kontinentales Tiefbohrprogramm; Althaus et al., 1984), and the continental seismic reflection program, DEKORP (Deutsches Kontinentales Reflexionsseismik Programm; Bortfeld et al., 1985).

Deep drilling interest concentrated on two potential sites, both located within Hercynian crystalline basement complexes: the Oberpfalz (Upper Palatinate) in eastern Bavaria and the Schwarzwald (Black Forest) in southwestern Germany. In both areas comprehensive efforts have been made to apply all kinds of geoscience investigations (Alfred-Wegener-Stiftung, 1985) for reconnaissance studies. Reflection measurements were organized within the framework of the DEKORP. In this paper we describe the contribution of seismic methods to the understanding of structural and physical properties of the Hercynian crust beneath the Black Forest in conjunction with other geophysical sounding methods. The seismic survey consisted of four types of investigations:

A) Deep reflection profiling (near-vertical incidence; Sect. 3).

B) Deep refraction profiling (long range profiles; Sect. 4, 4.1).

C) Expanding-spread profile (ESP; Sect. 4, 4.2).

D) High-resolution methods (near-surface, borehole measurements; Sect. 3.4.2).

This article deals with programs A, C and D and with a combined reflection-refraction interpretation, using other geophysical data as well. Details of the refraction experiment B can be found in Gajewski and Prodehl (1987).

The reflection network was planned to get regional structural control from a 170-km-long NS profile and spatial control of the central Black Forest region from three shorter intersecting profiles. The NS profile 8401 follows approximately the morphological axis of the Black Forest crossing the Central Schwarzwald Gneiss Complex (CSGC), which is bounded in the west by the Tertiary Rhinegraben, in the north by the southward-dipping Saxothuringian-Moldanubian suture zone, in the south by the NW-dipping "Badenweiler-Lenzkirch" crustal thrust zone and in the east by gently eastward-dipping Mesozoic sediments (Fig. 1). Two other profiles (8402, 8403) are focussed on the proposed drilling area. A fourth supplementary line (8514) was planned to study the tectonic significance and lateral extent of the "Badenweiler-Lenzkirch" zone. The profile net is connected with reflection profiles in the south (Finckh et al., 1986) and in the east (Bartelsen et al., 1982; Walther et al., 1986).

The field and processing parameters were chosen to provide good resolution throughout the entire crust. In order to link the crustal seismic sections to surface structures for their geologic-petrological interpretation, we performed

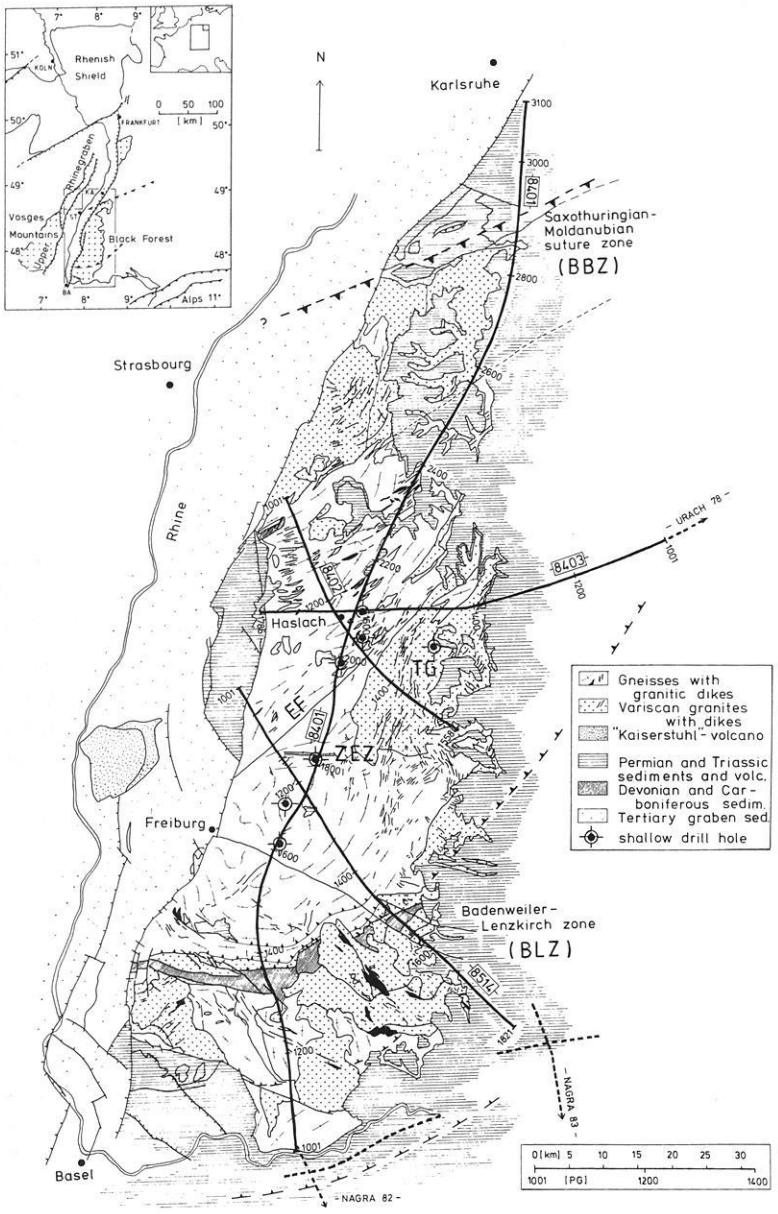

Fig. 1. Geological-tectonic map of seismic reflection profiles 8401, 8402, 8403 and 8514. The Central Schwarzwald Gneiss Complex is bounded by two Hercynian thrust zones: the Baden-Baden zone (*BBZ*) in the north (Saxothuringian-Moldanubian suture zone) and the Badenweiler-Lenzkirch zone (*BLZ*) in the south. *ZEZ* Zinken-Elme zone, *TG* Triberg Granite, *EF* Elztal Fault, *PG* geophone location

near-surface high-resolution measurements at selected sites and a systematic evaluation and tomographic inversion of first arrivals of the reflection recordings. From the interpretation of the refraction data, an outline of the two-dimensional velocity structure of the Black Forest emerged. Additional velocity information of the target area and further constraints on the physical nature of the crust were established by intensive one- and two-dimensional seismic modelling of reflection and refraction data and by an expanding-spread profile (ESP) focussed on the central Black Forest.

In the past, intensive geophysical studies in the region concentrated mainly on the Rhinegraben. Results of these studies, in particular of the seismic investigations, are documented in, e.g. Illies and Mueller (1970), Illies and Fuchs (1974), Edel et al. (1975), Prodehl et al. (1976), Illies (1981) and Zucca (1984). Fuchs et al. (1987) opened a new phase of discussion on the properties and evolution of the lower crust beneath the Rhinegraben system, relating seismic reflection results in the Rhinegraben proper (Dohr, 1970) with corresponding results described in this paper.

2 Geological and petrological environment

The Black Forest is the uplifted eastern shoulder of the Rhinegraben rift, where rocks of the Hercynian basement complex of Central Europe are exposed.

The structural zonation of the European Hercynian fold belt is described in Behr et al. (1984). It is subdivided into two external zones and one internal crystalline zone. The external Rhenohercynian and Saxothuringian zones consist of Paleozoic sedimentary rocks, volcanics and a minor proportion of crystalline blocks.

The Black Forest and Vosges are part of the internal Moldanubian zone which consists of Precambrian and Paleozoic terranes accreted during the Acadian/Hercynian orogenic cycle between the southern continent, Gondwana, and a northern continent, N. America-Europe. Thrust belts formed north and south of the internal crystalline zone. The northern belt (Saxothuringian zone, northern part of the Armorican Massif) is characterized by NW vergence of the major structures, whereas the southern belt (Mora-

vian zone, Southern Central Massif, Southern Armorican Massif) shows SE- and S-directed vergence.

During an early stage of the Acadian/Hercynian orogenic cycle, oceanic crust was subducted along both mobile belts. This event was followed by continent-continent collision in Carboniferous time (Lorenz and Nicholls, 1984; Matte, 1986). The later stage is characterized by complex wrench faulting and extensional tectonics of Basin-and-Range type.

The crystalline basement of the Black Forest consists of high-grade gneisses and migmatites intruded by Hercynian granitoids. The Paleozoic Badenweiler-Lenzkirch zone separates two crystalline blocks: the Central Schwarzwald Gneiss Complex (CSGC) and the Southern Schwarzwald Complex (SSC), which differ significantly both in their petrological and geophysical characteristics.

The CSGC consists of intensely deformed and transposed metapsammitic and metapelitic gneisses of Precambrian age.

The high-grade gneisses and migmatites of the basement complex (CSGC) display a polyphase metamorphic evolution. Numerous small bodies of eclogites (or eclogitic amphibolites), ultramafics (both spinel- and garnet-bearing serpentinites and pyroxenites) and granulitic gneisses indicate older high- and medium-pressure metamorphic events (Klein and Wimmenauer, 1984; Wimmenauer and Adam, 1985).

The Hercynian tectonic evolution of the CSGC can be documented along two NE- to ENE-trending belts of strongly deformed Paleozoic sediments and volcanics: the Baden-Baden zone in the north and the Badenweiler-Lenzkirch zone in the south. These zones represent thrust faults opposed to each other with northwestward and southeastward vergences. The Baden-Baden zone is regarded as the boundary between the Moldanubian and the Saxothuringian zone of the Hercynian fold belt. NW-directed tectonic transport is indicated by transposed foliations in weakly metamorphosed sediments which dip to the SE beneath higher-grade micaschists and gneisses. Overthrusting was followed by dextral strike-slip motions along this zone. The Badenweiler-Lenzkirch zone separates the Central Schwarzwald Gneiss Complex from the Southern Schwarzwald Complex. SE-directed tectonic transport is indicated by a 2- to 4-km-wide, strongly deformed WE-striking zone of Paleozoic sediments, metasediments, volcanics and mylonitic gneisses which dip to the NW beneath the CSGC. Sporadic fossils indicate that sedimentation occurred between around 370 and 335 Ma. In this time span the sedimentary environment changed from deep-water deposition to shallow marine and continental sedimentation (Sittig, 1969). This may be the result of considerable tectonic shortening in this time span. The mylonites and inverse metamorphic isograds demonstrate overthrusting of the hanging-wall CSGC over the sedimentary sequence to the SE. As in the Baden-Baden zone, thrust movements were followed by strike-slip motions. Within the CSGC, further convergent zones exist (e.g. Zinken-Elme zone).

Hercynian crustal evolution culminated with the emplacement of several suites of granitic plutons mostly of S-type character, the oldest of which show penetrative mylonitic/cataclastic deformation (370–335 Ma). The suite of the syn- to post-tectonic granites covers a time span of more than 70 Ma (370–290 Ma). Structural and geochemical investigations reveal the evolutionary trends both in time and space of the various granite suites (Emmermann, 1977). Ignimbrites and rhyolites of Permian age mark the final stage of the Hercynian magmatic activity (Lippolt et al., 1983).

Late-Carboniferous to Permian intramontane troughs filled with clastic sedimentary rocks and extrusive magmatic activity indicate a change in tectonic style towards extension of the Hercynian basement during this time. Within the basement, the pattern of late-Hercynian extension is indicated by porphyric and lamprophyric dikes and by post-metamorphic cataclastic deformation within the CSGC, the SSC and within the granite plutons.

In Mesozoic time, subsidence of platform type is characterized by non-marine redbeds and shallow marine epicontinental deposits.

Due to the stress regime in the foreland of the Alpine collision zone, a system of grabens formed in the early Tertiary. Subsidence in the Rhinegraben started at 45–40 Ma. Uplift of the graben shoulders of more than 2000 m caused exposure of the Hercynian basement. Related to the rift event, the Moho rose to extremely shallow depths by updoming in the southern Rhinegraben, where a depth of 24 km is shown by intensive seismic refraction studies (Edel et al., 1975).

A specific goal of the seismic sounding was to clarify the role and extent of Hercynian thrust and extension tectonics for the entire Black Forest region and, in particular, for the central Black Forest area.

3 Seismic reflection profiling and structural image

For economic reasons and difficult terrain and permitting conditions we decided to use the Vibroseis technique, bearing in mind the convincing results of the COCORP (USA) and ECORS (France) programs for crustal reflection profiling. Explosive sources were used in additional wide-angle measurements with equipment of various research institutions, in order to get velocity control (Sect. 4).

The general goal of the geophysical reconnaissance program was to collect all kinds of data for a long N–S crustal section. Consequently, the N–S reflection profile was regarded as a key profile for studying the regional geological and tectonic setting of the Black Forest. Since COCORP started deep crustal reflection profiling in 1975, it has been demonstrated that profiles at least 100–200 km long are necessary to identify the structural-tectonic style of a crustal segment. Profile 8401, therefore, follows the morphological axis of the Black Forest along 170 km across the Central Gneiss Complex and the adjacent thrust zones: "Baden-Baden" in the north and "Badenweiler-Lenzkirch" in the south (Fig. 1). At the southern end the line joins the reflection network of northern Switzerland (Finckh et al., 1986). For three-dimensional structural control, the central target area was covered by two intersecting profiles generating a triangle of 3–4 km side length together with line 8401. Profile 8402 is about 45 km long and traverses the crystalline basement almost perpendicularly to the Hercynian strike. Profile 8403 is a prolongation of the Urach profile U 1 (Bartelsen et al., 1982) forming a 120-km E–W transect, roughly perpendicular to the Rhinegraben. It will be extended into France in 1988, crossing the Rhinegraben and the Vosges mountains, as a joint ECORS-DEKORP program.

These three profiles, 8401–8403, with a total length of 278 km were accomplished in a 3-month campaign in 1984.

Table 1. Acquisition parameters

Source	5 vibrators VVDA (14 t) on profiles 8401, 8402, 8403 and VVEA (19 t) on profile 8514	
	spacing between vibrators	20 m (8514: 10 m)
	moveup between sweeps	6 m (8514: 2 m)
	total source array length	146 m (8514: 48 m)
	vibrator point (VP) spacing	80 m (8514: 40 m)
	signal	upsweep 12–48 Hz, logarithmic, duration 20 s
	no. of sweeps per VP	12 (8514: 5)
	in-line offset	2×200 m
	max. off-line offset	700 m
Receiver	no. of geophone groups	200
	group spacing	80 m
	spread length	16.24 km
	spread	split spread (8514: asymmetric)
	no. of geophones (10 Hz) per group	24
	pattern	in-line, weighting uniform
	spacing between geophones	3.5 m
	total array length per group	80 m
Recording	equipment SERCEL 348 (8514: SERCEL 368), telemetric, automatic noise reduction before correlation, correlator-stacker CS 2502	
	traces	200
	correlation before vertical stack, sampling rate	4 ms
	total recording time (uncorrelated)	32 s
	correlated record length	12 s
	vertical stacking of correlated records	12-fold (8514: 5)
	preamplification	$2^7 = 42$ dB
	low-cut filter	12.5 Hz
	high-cut filter	62.5 Hz
Coverage	reflection	max. 100-fold
	refraction	max. 200-fold (8514: 400-fold)
	CDP spacing	40 m (8514: 20 m)

A fourth profile, 65 km long (8514), was recorded in order to investigate prominent reflectors of profile 8401 in the upper crust in greater detail, particularly the northward-dipping Paleozoic "Badenweiler-Lenzkirch" thrust zone (BLZ) and its implications for the proposed drill site near Haslach (Fig. 1). This profile was recorded in November 1985.

3.1 Field survey

The field work was performed by a Vibroseis crew of the Prakla-Seismos AG company, Hannover. The routine oil-and-gas exploration crew was supplemented by additional vibrators, trucks and personnel recruited from the University of Karlsruhe who assisted in the weathering survey, in static corrections, geological mapping and in other crew operations. The total crew consisted of 57 persons and about 30 trucks, all operating within a range up to 40 km.

The field parameters (Table 1) were chosen to meet the following conditions: a multifold horizontal coverage of about 100 [as estimated from a comparative Vibroseis-explosion test on profile DEKORP 2-S; Bortfeld et al. (1985)], a CDP spacing of 40 m and a daily progress of 4–5 km; i.e. a 200-channel recording system along a 16-km spread with 80-m source and geophone group spacing had to be utilized. A symmetric split-spread with 200-m in-line offset was chosen to increase the shallow coverage and resolution. Upper-crustal resolution and velocity control by normal move-out require different spread configurations. We decided in favour of structure resolution (split-spread), while velocity control was achieved separately by an expanding-spread profile (Sect. 4.2) and by a refraction experiment also along the main N-S line [Gajewski and Prodehl (1987) and Sect. 4.1]. A source pattern of five vibrators and 146 m length, with 10- to 12-fold vertical stacking, yielded reliable suppression of groundroll noise. A 12- to 48-Hz upsweep of 20 s length was chosen, based on a start-up test. The received signal was filtered and digitized at each geophone group consisting of an 80-m in-line array of 24 geophones and a remote box. The data were then multiplexed and telemetrically transmitted to the recording truck by a 16-km-long cable. Automatic noise rejection and full precision correlation were applied before 12-fold vertical stacking and storage on magnetic tapes.

In contrast to the explosion technique, the Vibroseis method allows choice of bandwidth of the emitted signal. In practice, however, vibrator-ground interaction may influence the spectral content of the seismic signal, depending on mechanical properties of the vibrator system and elastic properties of the ground. During the Vibroseis survey, daily similarity tests were performed under different geological and coupling conditions. The baseplate signal can be regarded as seismic source signal (Lerwill, 1981). The amplitude spectra of the similarity recordings were compared with the spectra of the field recordings acquired at the same vibrator locations. In Fig. 2 four examples are shown to demonstrate the ground-dependent differences between amplitude spectra of the pilot signal (12–48 Hz), baseplate signals of five vibrators, and five seismogram portions of 0.5 s length at different recording times.

The upper example shows an ideal broadband source spectrum, which is similar to the pilot signal showing the normal situation in the crystalline area of the Black Forest. In the other three examples of Fig. 2 resonant frequencies appear, which in most cases are low above thick Permian and Triassic sediments and high on paved roads. The stu-

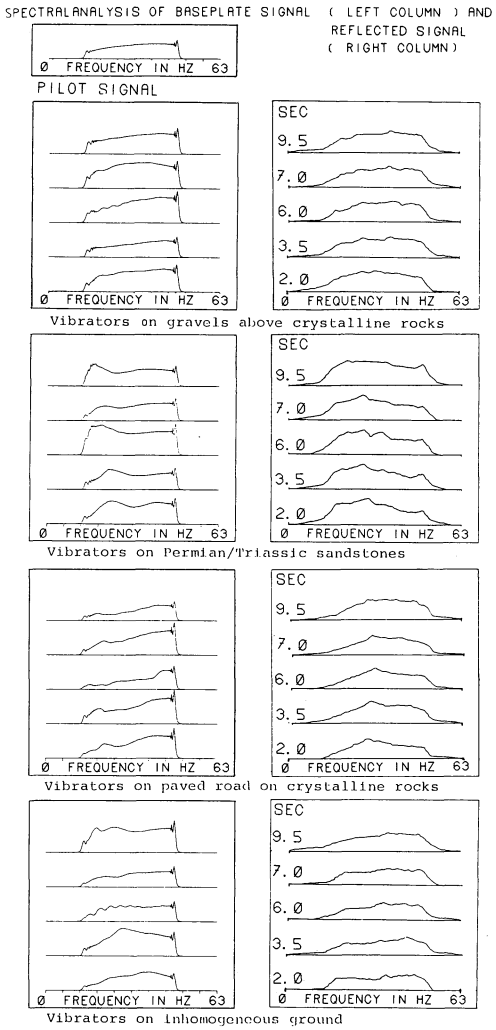

Fig. 2. Spectral analysis of baseplate signals of five vibrators from similarity tests (*left panels*) and of corresponding seismic records (*right panels*; sum spectra of high S/N ratio traces from five 1-s time sections starting at TWT indicated on left-hand side). Amplitudes are normalized, scales are linear. Pilot signal (upsweep, 12–48 Hz, 20-s length) *on top*

dies of Vibroseis source characteristics showed that mainly broadband seismic signals resulting from favourable vibrator-ground interactions were emitted.

A detailed study of vibrator-ground interactions has been carried out by Schnell (1987), who considered the influence of the road and the near-surface geology.

3.2 Data processing

The data processing for Black Forest profiles was carried out at the DEKORP Processing Center, Institut für Geophysik, Technische Universität Clausthal. Details and problems of the processing sequence have been discussed by Bortfeld et al. (1985) regarding the DEKORP profile 2-South. True-amplitude and crooked-line processing were applied routinely and post-stack coherency-filtering optionally. The high signal/noise ratio, even in the common source gathers, is shown in Fig. 3.

Common midpoint (CMP) sorting took crooked-line geometry into account. A lateral deviation of vibrator points of up to 700 m due to terrain conditions and a slightly bent receiver line required crooked-line processing, for which a processing line through the centre of the midpoint distribution was defined.

Stacking-velocity analysis was based on visual inspection of constant-velocity stacks of groups of 20–50 CMPs using 28 velocities in the range 4000–9760 m/s. Often, the picking of optimum velocities was hampered by the lack of continuous reflectors in the upper crust. There the quality of stacked sections could often be enhanced by unconventional, high stacking velocities (see also Sect. 6).

Figures 4–6 illustrate the different character of imaging by AGC (automatic gain control) stacking, TA (true amplitude) stacking and FD (finite difference) migration and their specific advantages, chosen from the central part of profile 8401.

For interpretational purposes, all processing modes were taken into account in order to exploit the special advantages of each section. The stacked sections reveal a better signal/noise ratio and often a better readability than the migrated sections. The AGC-stacked data, even the weaker elements whose amplitudes are below the ambient noise level, make reflections visible mostly by their coherence. The TA-stacked data allow a good estimate of the real amplitude differences and reflection coefficients. On the other hand, they show a rather heterogeneous quality within the first 2 s TWT due to varying coupling conditions at the surface.

Migration corrects for structural distortions by focussing diffractions and moving dipping events to their real location. Migration often produces artificial effects known as "smiles", especially in the deeper parts of the sections (Warner, 1987); therefore, three-dimensional control by the intersecting profiles is essential for reliable interpretation of the data.

Migration velocities were based on smoothed stack velocities. In addition to finite-difference migration, constant-velocity migrations were applied on selected portions. A high-amplitude event at a midcrustal level, which shows clear diffractions at each side, was used as a test object for migration efficiency. Based on imaging-time variation (De Vries and Berkhout, 1984), migrated sections for different migration velocities were generated in one single, recursive downward-continuation process (Fig. 7). The variation between 6220 and 5090 m/s shows that the migration process for these data is rather insensitive to velocity variations. Using the criterion of optimal focussing we determined 5700 m/s as the maximum velocity for this particular data set.

3.3 Presentation of data

Figure 8 shows a compilation of structural information obtained by the complete profile net, based on migrated sections presented as simplified line drawings.

Each line or reflection event does not necessarily represent a first-order discontinuity. Laminated zones, with a thickness below the seismic wavelength, increase the reflectivity by constructive interference of multiple internal reflections in certain frequency bands (Fuchs, 1969). The crustal structure image is dominated by a strong differentiation into a highly reflective lower crust of laminated character, between 5 and 9 s TWT, and an upper crust of lower reflection density. Figure 9 shows a selected seismogram close-up from the TA-stacked profile 8401 which demonstrates this

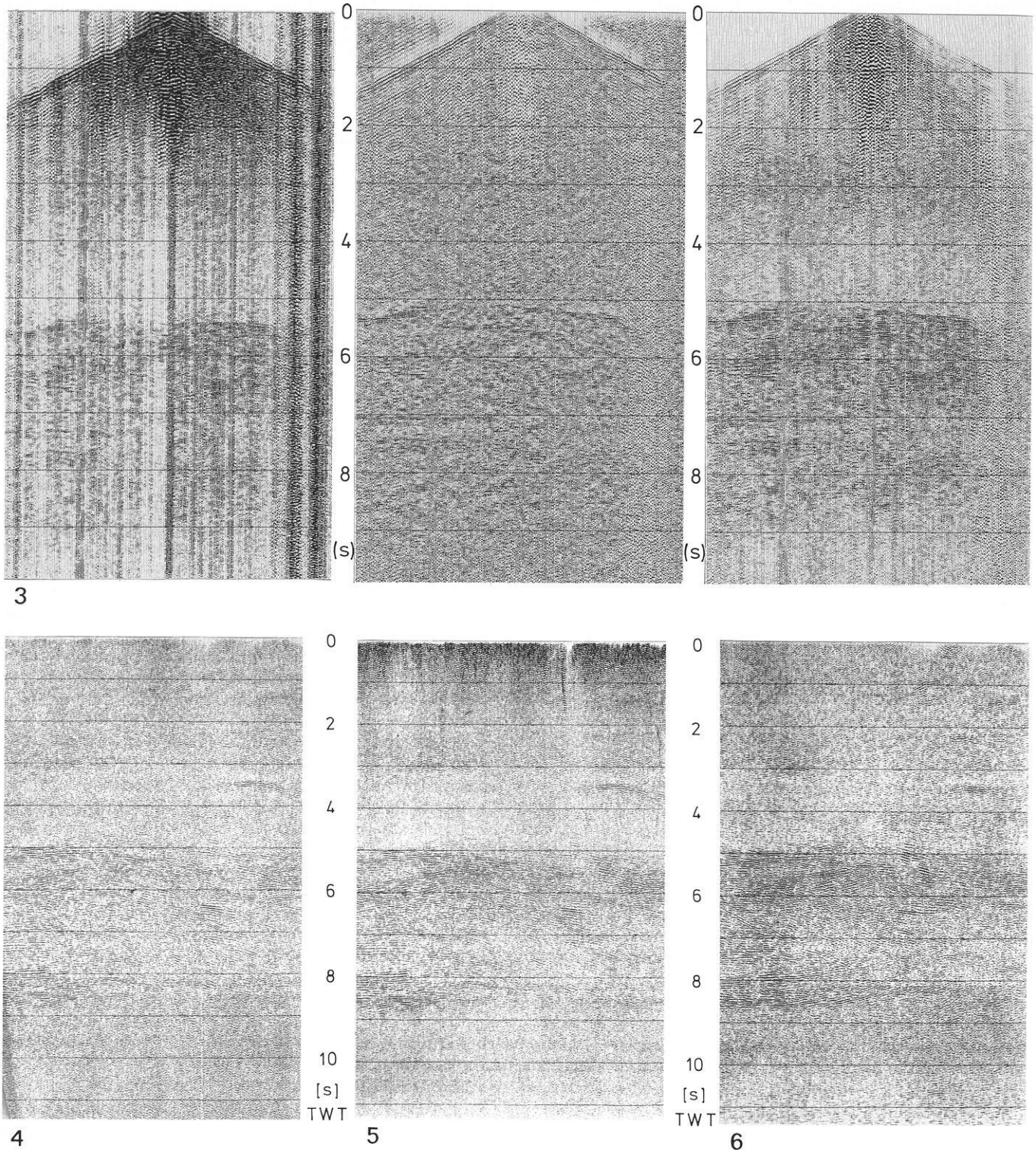

Fig. 3. Examples of common source gathers (profile 8401, *VP* 2178) in three different display and scaling modes. *Left:* original field recording without further processing; *middle:* AGC (automatic gain control)-scaled record after application of static corrections; *right:* TA (true amplitude) record. TA includes horizontal trace equalization and amplitudes are multiplied between 0 and 3 s TWT by kTe^{aT} (k constant, T travel time, a constant of absorption) to compensate for spherical divergence and absorption. The values have been assessed empirically in order to obtain a balanced seismogram. Note the strong reflections from the lower crust beginning at 5 s TWT (two-way travel time), even in single-fold seismograms. Length of spread = 16.24 km

Fig. 4. Example of a conventional AGC stack from the central part of line 8401. Note the balanced energy which is determined from a moving time window of 500 ms. Frequency filtering, bandpass characterized by lower stop – pass band frequency/upper pass – stop band frequency: 0.0–2.4 s TWT – 14–20/37–48 Hz; 2.4–4.4 s TWT – 11–18/37–48 Hz; 4.4–12.0 s TWT – 8–15/37–48 Hz. Length of section = 22.4 km

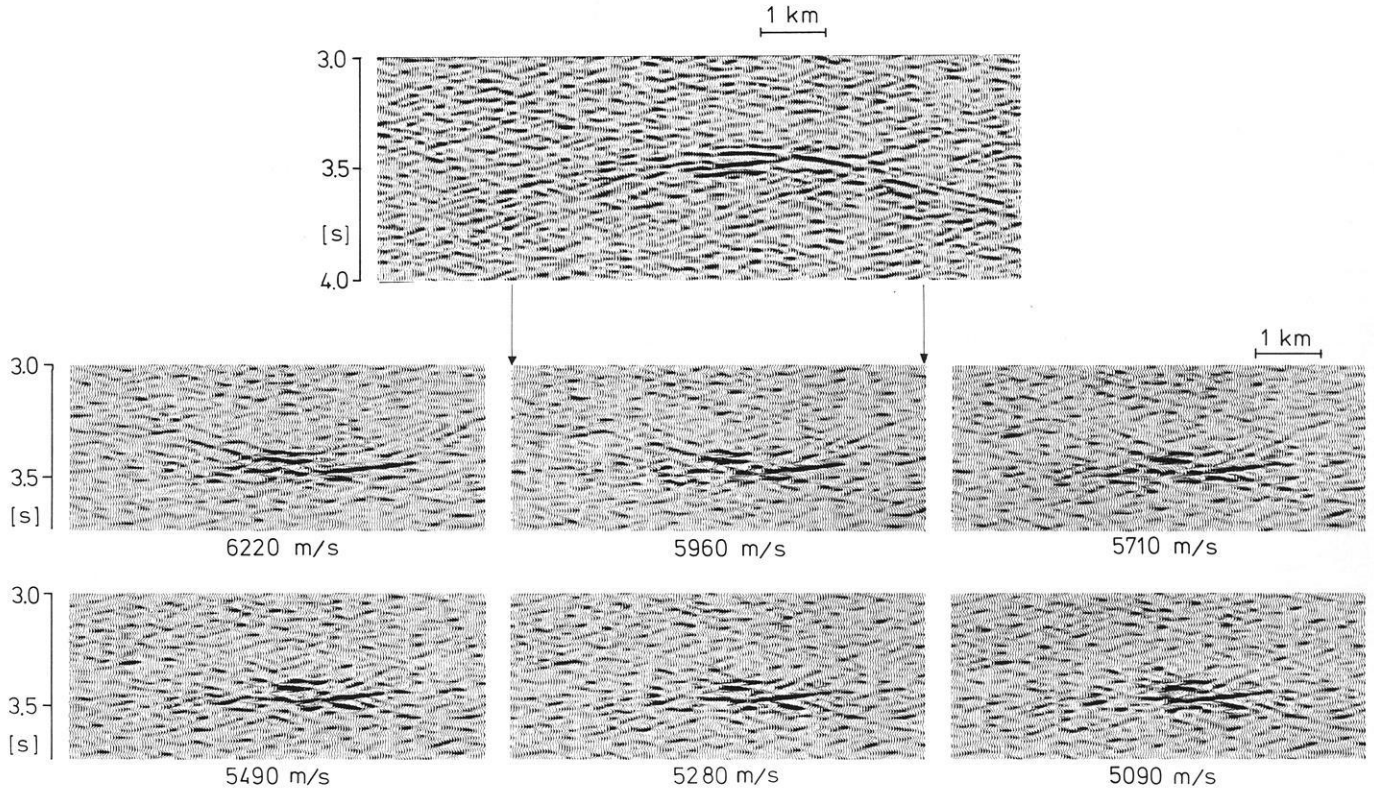

Fig. 7. Constant-velocity migrations of a high-amplitude event (bright spot) beneath Haslach (location 2070 of line 8401). Using the criterion of optimal focussing, the migration velocity of approximately 5700 m/s may be regarded as the maximum acceptable value

contrast. The lower part of the upper crust all over the profile net is characterized by a mostly transparent zone. The top of the laminated lower crust was found at an almost constant level of 5 s TWT, corresponding to a depth of 14 km with small undulations. The reflective character of the lower crust breaks down abruptly at about 8.5 s TWT, corresponding to a depth of 25.5 km with slight undulations and a relative updoming beneath the Kirchzarten basin (location 1600, 8401). This observation leads us to define the crust-mantle boundary by the deepest continuous reflectors, and which coincides with the conventional Moho defined by refraction seismics (cf. Sect. 4.1 and 7). The upper mantle is the most transparent part in the seismic sections. No significant reflection signals could be identified within the last 3 s of recording time; maximum time was 12 s, corresponding to a maximum depth of approximately 36–38 km. Figure 10 shows an example from profile 8514 which demonstrates the abrupt change of the reflectivity pattern at the Moho.

The lower crust is widely characterized by horizontally layered reflections, which are sometimes consistent over 10–20 km, with some discordant patterns of dipping elements. Smiles appear at some deeper locations: in the central part of profile 8401 (Fig. 6) and in the southeastern part of profile 8514 (Fig. 11). Locally, the lower crust also contains transparent patterns above the Moho: for instance, in the southern part of profile 8401, at location 1500 of profile 8403 and in the northwestern part of profile 8514. Between locations 2300 and 2500 of profile 8401 (Fig. 8) the reflection energy fades out throughout the whole crust. This is probably caused by scattering of seismic energy due to an accumulation of vertically arranged fractures and dikes in the upper crust, rather than due to disturbances during data acquisition. The laminated lower crust was intensively modelled (Sect. 5) in order to derive physical constraints for petrological interpretations.

The upper crust contains mostly dipping, often crosscutting and high-amplitude events of local character. At the northern end of profile 8401 the Rotliegend trough appears in the seismic section with some internal formations and vertical faults. In this sedimentary basin the frequency content of the seismic signals is reduced so that the laminated character of the lower crust cannot be resolved. Seismic stripping and long-term statics (cf. Sect. 3.4.1) can improve the data quality beneath the Permian sedimentary basin. In the middle and lower crust at the northern end of line 8401 a pattern of southward-dipping reflectors is clearly visible (Figs. 8 and 9); only a few reflectors penetrate the horizontally layered crust-mantle boundary. This may be a relic feature of a Hercynian thrust, possibly the Saxothur-

Fig. 5. TA stack corresponding to the section of Fig. 4. This section gives a better estimation of true reflection energy, but is of rather heterogeneous quality within the first 2 s TWT due to varying coupling conditions of detectors and sources and varying ambient noise. A horizontal scaling is included, normalizing the trace energy between 3.5 and 12.0 s TWT

Fig. 6. Finite-difference migration based on the AGC stack of Fig. 4. The curved reflector pattern in the deeper part of the section is partly due to sideswipe. The majority of these elements correspond to true dipping reflections controlled spatially by the intersecting lines 8402 and 8403

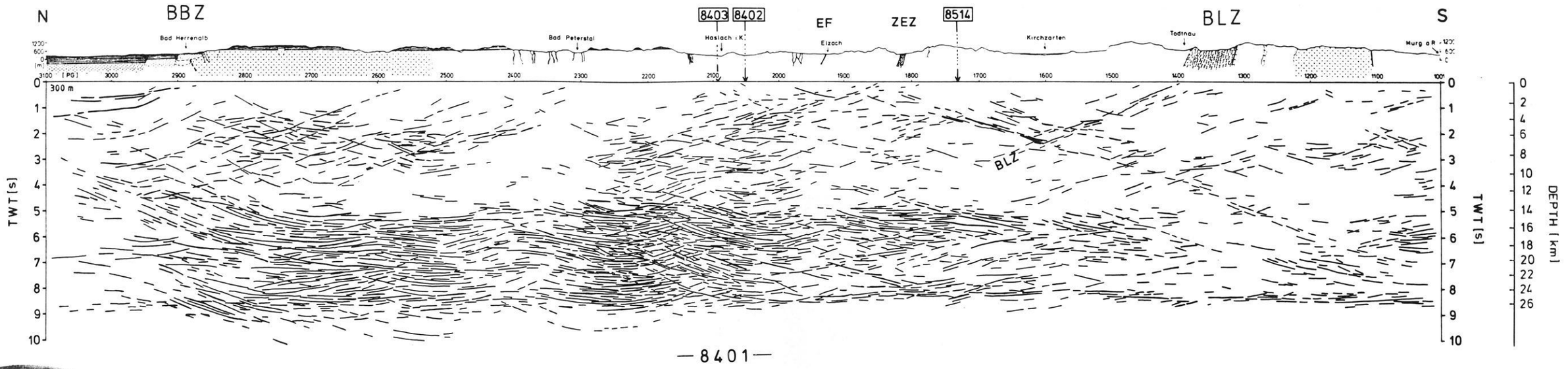

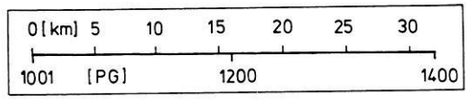

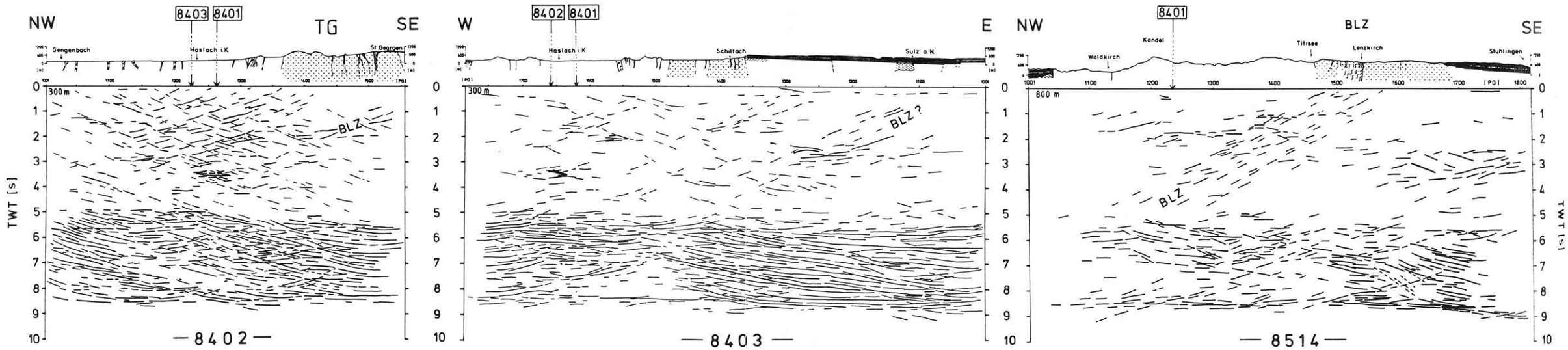

Fig. 8a. Line drawings for profiles 8401, 8402, 8403 and 8514, based on migrated sections. Lines correspond to coherent phases. The depth scale at the right-hand side of profile 8401 is derived from wide-angle data. *BBZ* Baden-Baden zone, *BLZ* Badenweiler-Lenzkirch zone, *EF* Elztal Fault, *TG* Triberg Granite, *ZEZ* Zinken-Elme zone, *PG* geophone location

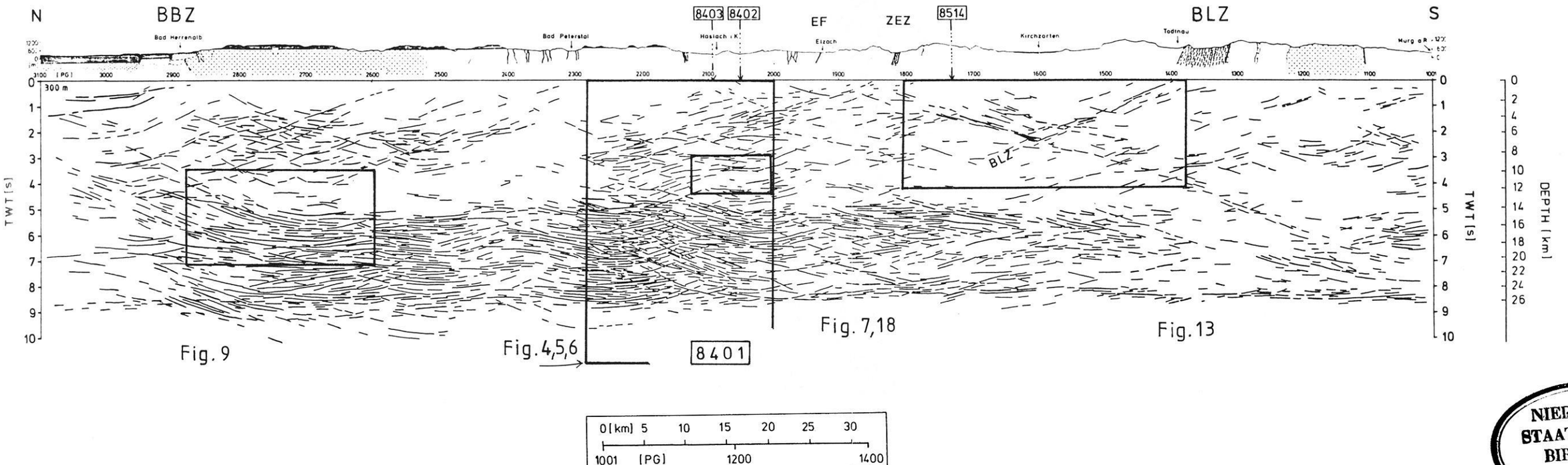

Fig. **8b.** Same as Fig. 8a. Positions of seismogram sections presented in Figs. 4–7, 9–14 and 18 are marked

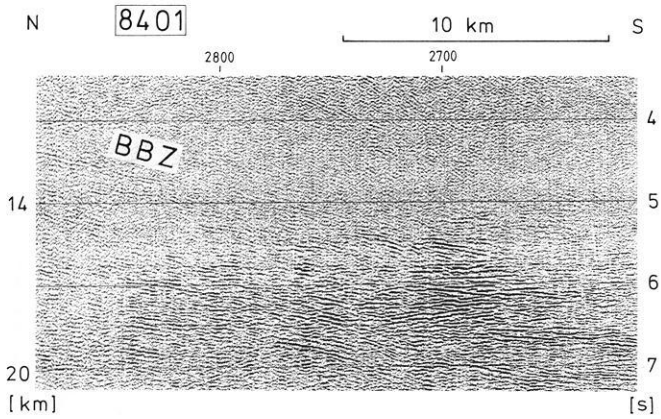

Fig. 9. Section of the TA stack from the northern part of line 8401 showing strong differentiation between the highly reflective lower crust, beginning at about 5 s TWT, and the transparent middle crust. The dipping element on the left (4–5 s TWT) may be related to the Baden-Baden thrust zone

ingian-Moldanubian suture zone of the Hercynian belt, also called the Baden-Baden zone (BBZ, Sect. 2). Further to the south, particularly in the Central Schwarzwald Gneiss Complex, a criss-cross pattern of low-angle reflectors prevails in the upper crust (compare seismogram close-ups in Figs. 4 and 5 for profile 8401 and Fig. 12a and b for profile 8402). In this area cataclastic shear zones dipping to the SE are found at the surface and which are identified as reflectors by high-resolution seismics (Sect. 3.4.2). These SE-dipping reflectors of the upper crust are interpreted as late-Hercynian extensional faults. On the other hand, north- and northwest-dipping reflectors of the criss-cross pattern can be correlated with mylonitic, ductile deformation zones associated with intraplate convergence and thrust zones of Hercynian age in the southern Black Forest (Zinken-Elme zone, ZEZ, and Badenweiler-Lenzkirch zone, BLZ).

The BLZ is a relic of a major Hercynian thrust and can be traced clearly on profiles 8401 and 8514. It dips N to NW, down to a depth of 10–12 km (Fig. 13 from profile 8401, Fig. 14 from profile 8514), and intersects or is intersected by another reflector. This Glottertal reflector cannot be traced clearly to the surface. It shows the strongest reflection amplitudes observed in the upper crust of the Black Forest. From profiles 8401 and 8514, its strike is determined to be parallel to 8514 and its dip to be to the SSW. It is probably an extension fault related to corresponding shear zones of normal-fault character and Hercynian origin which were mapped at the surface. Recently collected seismicity data demonstrate that this reflector represents an active fault (Bonjer et al., 1986), indicating that the present stress field is released along ancient structures. Hence, brittle deformations may be responsible for the pronounced Glottertal reflections.

The criss-cross pattern of low-angle reflectors reveals that low-angle convergent and divergent structures contribute a much greater deal to the architecture of the crust than previously assumed. In accordance with geological findings (Sect. 2 and 7.2), we believe that thrusts penetrating the entire crust are overprinted by low-angle normal faults in the upper crust and by a strong horizontal 'lamination' in the lower crust, including the crust-mantle boundary. Alternatively, such an irregular pattern could be influenced by strong shallow velocity inhomogeneities which tend to smear out individual reflections into a complex pattern (Peddy et al., 1986). However, the persistence and continuity of lower-crustal reflectors indicate that a strong influence of distortions in the upper crust can be excluded.

3.4 Special investigations

3.4.1 Velocity structure from first arrivals. First arrivals and subsequent refracted arrivals, as well as surface waves, are systematically eliminated by the muting procedure in standard reflection data processing. This causes a lack of coverage and structural information in the topmost part of the seismic section, mainly within the first 0.5 s TWT corresponding to a depth of about 1 km. To compensate for this loss of information, the first arrivals were evaluated separately to determine in detail the lateral variation of

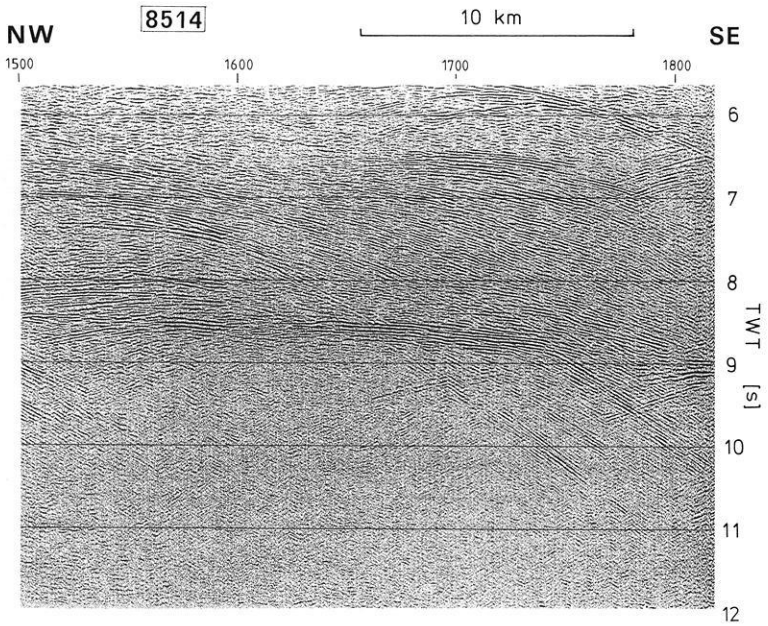

Fig. 10. Stack section from the southeastern part of line 8514. Note the strong reflections in the lower crust and, in particular, the strong continuous reflection from the crust-mantle boundary. This section is dominated by diffractions, even for more than 9 s TWT, having their apices in the lower crust. Diffractions originating at the crust-mantle boundary (e.g. on the *right side*) indicate vertical steps or small-scale undulations

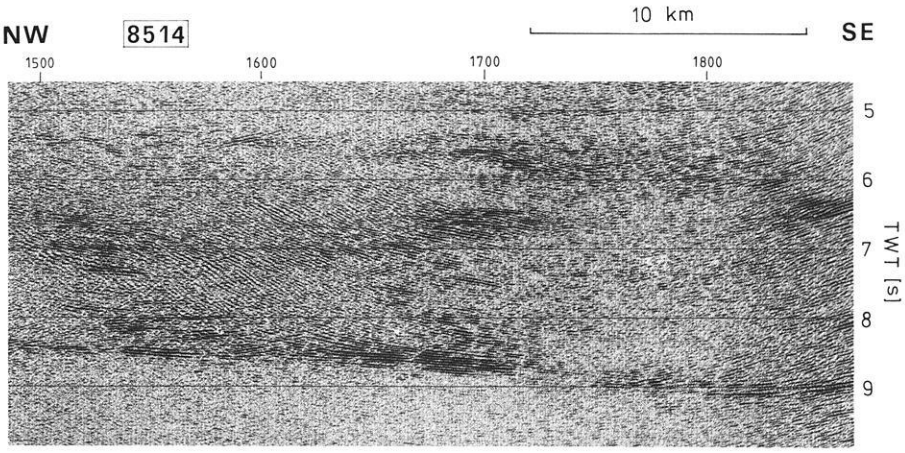

Fig. 11. Migration of stack section from Fig. 10. Note that deep diffractions are focussed mostly at their source structures. Also, migration produces artificial, curved elements (6–8 s TWT)

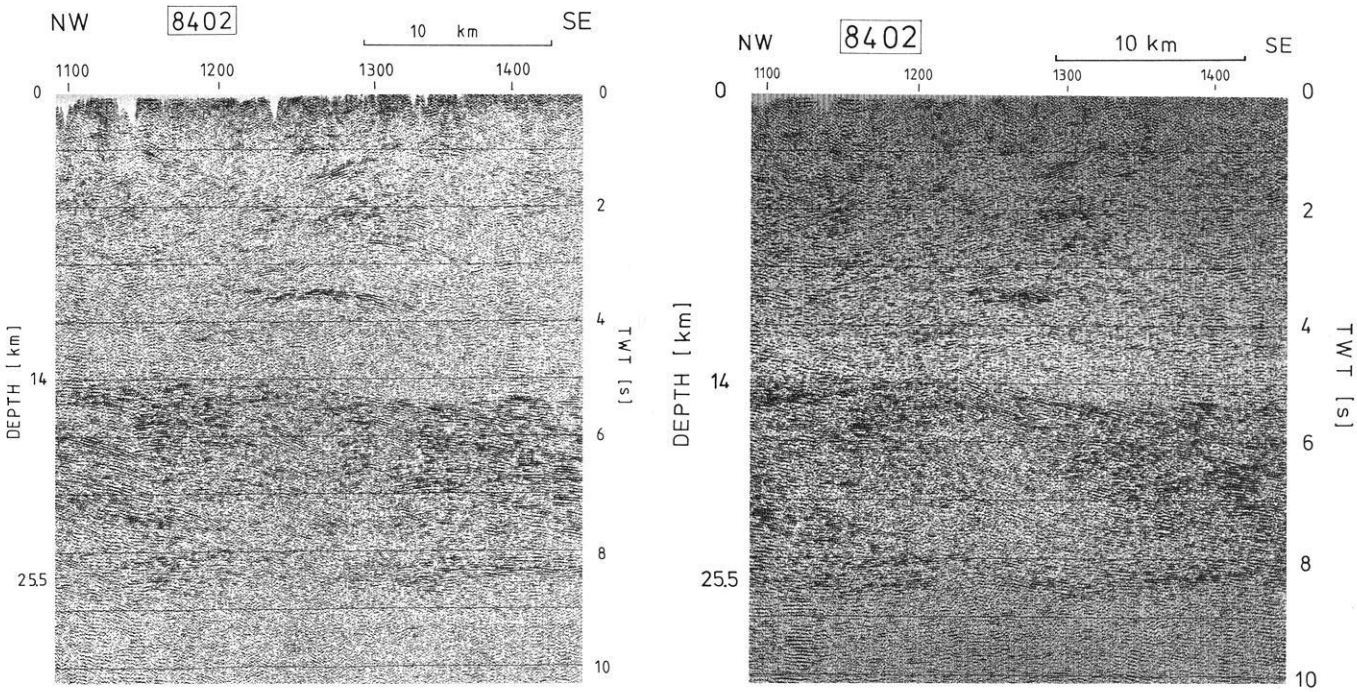

Fig. 12. Stacked section (*a*) and migrated section (*b*) of the central part of profile 8402 within the intersection area of profiles 8401–8403 near Haslach; bright spot at 3.5 s TWT

velocity structure for the upper 2 km. The refraction technique benefits from the extremely high data redundancy that reaches a maximum coverage of nearly 200 for each subsurface point.

The first arrivals of selected high-gain field records were picked manually and transferred to travel-time-distance plots. The "plus-minus" method of Hagedoorn (1959) was applied graphically to determine the laterally varying refractor velocity of the crystalline basement and its depth. Short refraction lines (weathering surveys) were carried out additionally at spacings of about 2 km to obtain information about the thickness and the velocity of the weathering zone and to control the intercept times and to calibrate the first arrivals of the Vibroseis data, since an in-line offset of 200 m of the Vibroseis split-spread geometry had to be bridged.

Basic static corrections were computed based on the results of the "plus-minus" method, topographic data and the interpolated results of the weathering survey. Statistical improvement of these static corrections (Fromm, 1984) was obtained by automatic evaluation of first arrivals. Short-period perturbations on the travel-time curves were transformed into delay times of the weathering layer, which were added to the basic corrections. Static corrections included an offset correction and were computed for a reference level of 300 m above mean sea level (profile 8514: 800 m).

Although surface rocks are composed of crystalline basement, gneiss or granite with occasional cover of a few metres of Quaternary deposits, the evaluation of the refraction data clearly shows a considerable thickness of low-velocity material varying between 2000 and 3500 m/s and with thicknesses between 50 and 300 m (see upper parts of sections in Fig. 16). This is probably due to lateral variations of rock weathering. The refractor velocity of the "solid" basement varies between 5000 and 5700 m/s. In Fig. 15 these velocities are related to different petrological assem-

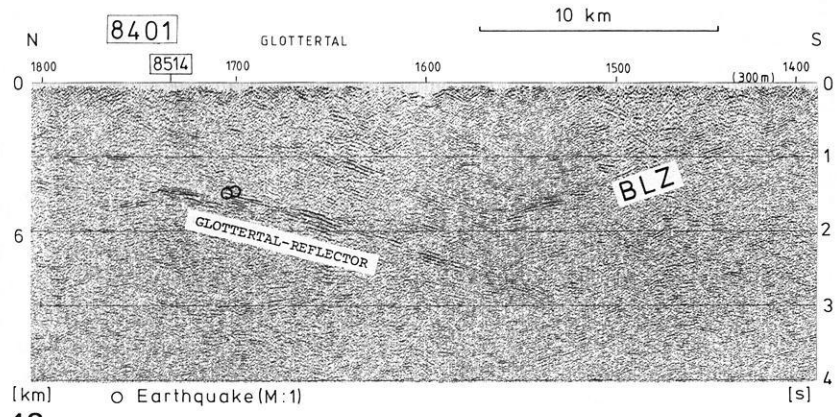

13

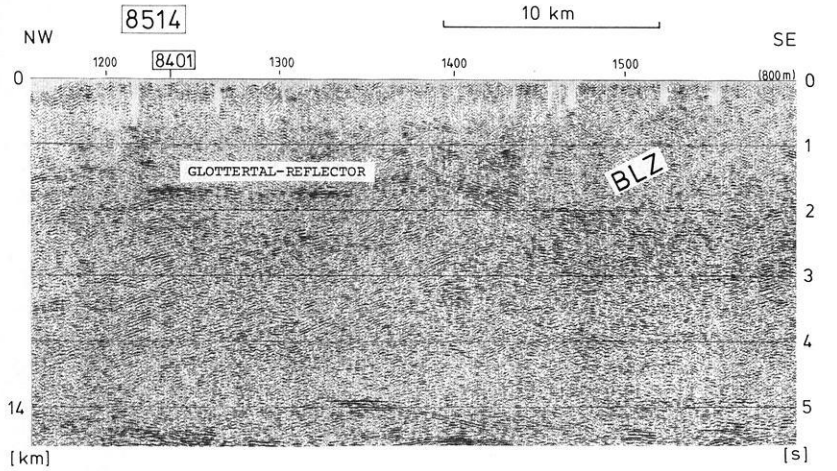

14

Fig. 13. Upper-crustal reflections from a southern part of the stacked line 8401. The northward-dipping elements on the right-hand side are connected with the Badenweiler-Lenzkirch thrust zone (*BLZ*). The southward-dipping prominent Glottertal reflector is interpreted as a low-angle normal fault. An earthquake sequence is located within this element (Bonjer et al., 1986). Precision of location is ±100 m. Focal mechanism is of shallow thrust type. Three-dimensional control is provided by the intersecting line 8514 (cf. Fig. 14)

Fig. 14. Part of the stacked profile 8514. The Glottertal and Badenweiler-Lenzkirch elements are delineated in a NW-SE direction allowing a reconstruction of dip and strike with the aid of profile 8401. The Glottertal reflector dips to SSW and strikes NW–SE. The surface trace of the *BLZ* is curved (cf. location map, Fig. 1). Its dip of about 30° can be followed to a depth of about 12 km

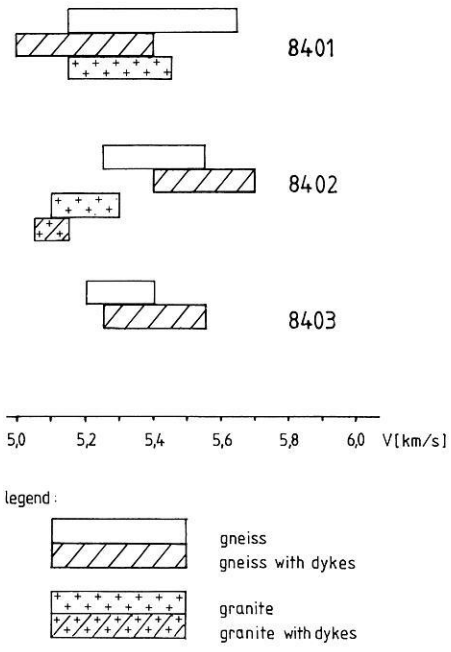

Fig. 15. Representative basement velocities for zone beneath weathering layer derived from first arrivals of Vibroseis field recordings. Length of bars corresponds to standard deviation of the mean values

blages which are documented by abundant exposures. Generally, granites tend to have lower velocities than gneisses. If associated with granitic dikes, both units show a relatively wide scattering of velocities. This might be explained by an azimuthal velocity dependence on the strike directions of the dikes with respect to the orientation of the profiles.

To investigate the velocity structure of the uppermost crust in greater detail, the complete set of first arrivals was picked by using the single channel algorithm (Ketelsen et al., 1983). This data set provides a maximum 200-fold coverage which is on average reduced to about 70- to 100-fold because of missing vibrator stations and missing picked values. The travel-time distance curves were inverted by different techniques (Giese, 1976; Slichter, 1932) yielding velocity-depth functions. As the most powerful and economical method, the maximum depth estimation method of Slichter (1932), making use of the triple data set comprising distance, travel time and apparent velocity, was used for preference.

Computations with synthetic, even laterally varying, models have demonstrated the reliability of this method. The high redundancy of velocity-depth data was used to smooth the velocity structure by averaging. Its reference level is the topography of the seismic basement (Fig. 16). A CMP-sorting technique (Gebrande, 1986) was applied but gave no further improvement. Another approach to control the velocity structure is the application of iterative

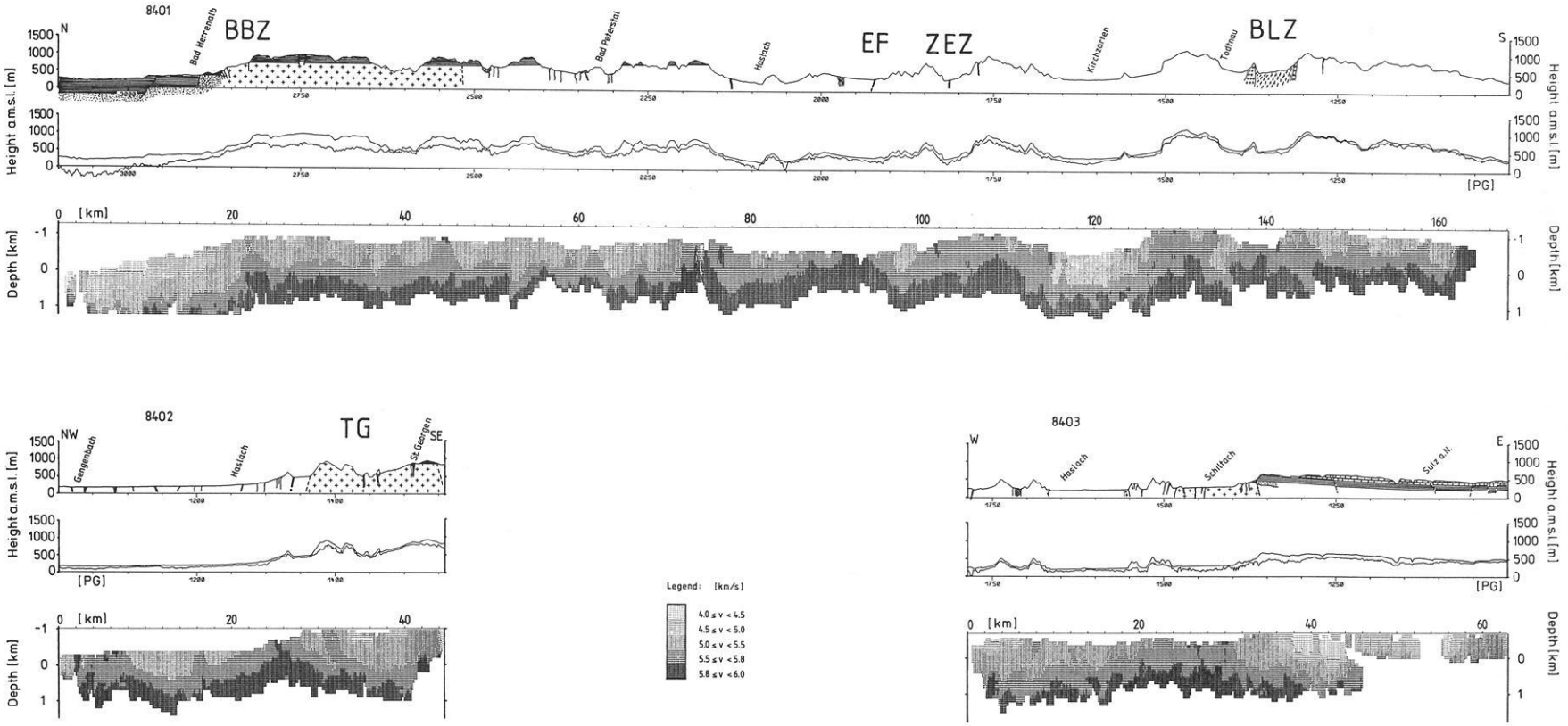

Fig. 16. Evaluation of the Vibroseis first arrivals for profiles 8401, 8402 and 8403. *Upper sections:* surface geology; *crosses:* granites; *white:* gneisses (with dikes); *other signatures:* Permian rocks and Paleozoic sediments of the Badenweiler-Lenzkirch zone. *Intermediate sections:* thickness of the weathering zone (heterogeneous, velocities of 2000–3500 m/s); *upper line* – topography, *lower line* – seismic basement. *Lower sections:* two-dimensional velocity structure of the basement. For velocities, see legend. Vertical exaggeration of topography is 4

tomographic methods (e.g. Gordon et al., 1970; Censor, 1983) which provide a velocity image directly from traveltime. The results correspond to those obtained by the Slichter-Method with only slight improvements (Rühl, 1987).

The velocity sections of Fig. 16 (lower parts) display considerable lateral variation of the velocity structure, ranging from 4000 to 6000 m/s. The lower velocities clearly correlate with a Permian and Triassic sedimentary cover in the northern part of profile 8401 and in the eastern part of profile 8403. Some conspicuous correlations between known petrological complexes are obvious. On profile 8401 higher-velocity material updomes in the core of the central complex of gneisses and anatexites. The section of profile 8402 reflects a significant velocity difference between the Triberg granite (5200 ± 100 m/s) and the gneisses (5400 ± 150 m/s, cf. Fig. 15) and a synclinal basin within the gneisses. High near-surface velocities at km 5 and 25 of profile 8402, km 25 of profile 8403, km 92 and 108 of profile 8401 correlate with belts of granulitic gneisses and mylonites (Hacker and Hirschmann, 1986).

In addition to geological interpretations, the assessment of long-term statics offers an important practical application. Based on the velocity model of Fig. 16, long-term effects of the order of 20–30 ms (comparable to a seismic period) were estimated within a CMP gather using a deeper reference level. These statics have not yet been applied to the data presented in this paper.

3.4.2 Seismic probing of near-surface crystalline rocks. One important but indirect approach to explain the nature of deep crustal reflectors is sophisticated modelling that estimates the physical parameters as described in Sect. 5.

As another approach, in-situ probing of seismic reflectors in crystalline rocks has been attained through geophysical logging tools and vertical seismic profiling (VSP) in a series of boreholes, and through their correlation with structures and lithologies of the cored rocks. The borehole studies were complemented by near-surface reflection and refraction profiles of high resolution in order to link deep seismic sections to known near-surface structures and lithology. Out of a great variety of seismic imaging tools and widespread resolution capabilities applied at different sites in the central Black Forest, two are presented in this paper.

For the investigations, a car-mounted high-pressure pneumatic hammer was used at 20-m intervals for generating compressional (*P*) waves and horizontally polarized shear waves (*SH*). Twenty-four receiver arrays of vertical geophones or, alternatively, horizontal geophones for *SH* recording, were deployed at 10-m intervals. Recording with a 24-channel digital signal-enhancement unit deployed in off-end geometry yielded a 6-fold coverage with CMP spacing of 5 m. The daily progress was 600–800 m.

First arrivals and refraction lines yield *P* velocities of 600 m/s (*SH*: 340 m/s) in the upper few metres and basement velocities increasing from 2800 to 4200 m/s (*SH*: 1700–2000 m/s) in the upper 50 m. In *P*- and *SH*-reflection sections near Haslach an interrupted reflection can be traced over the complete sections, dipping 30°–40° to the east. This reflection can be traced upward into a cataclastic zone related to a low-angle normal fault. This fault could thus be followed from the outcrop to a depth of about 700 m by this shallow reflection survey. Comparison with the deep reflection section 8402 (Sect. 3.3, Fig. 12) shows a continuation of this fault reflector to a system of reflectors which, dipping to the SE, penetrate the entire upper crust. We therefore interpret these and similar reflectors as indicators of late-Hercynian extension (cf. Sect. 7.2). However, in general, the shallow seismic sections show weak amplitudes and little consistency of reflectors, especially when using *SH* waves. This may be a consequence of complicated ductile folding and metamorphic transposition on a scale less than the seismic wavelength (*P*: 40–100 m, *SH*: 40–130 m), which might also account for the relative transparency and complexity of the entire upper crust.

Figure 17 shows an example for a data compilation for the "Hechtsberg" well (300-m depth) near Haslach. The original VSP record section displays the downgoing direct wave and the tube wave. The averaged *P*-wave velocity decreases from top to bottom from 5400 to 5100 to 4400 m/s, which is confirmed by the sonic log. This corresponds to a petrographic change (decrease of mafic constituents, decrease of degree of foliation) from orthogneisses to paragneisses. The upgoing wavefield delineates a sequence of reflections which can be correlated with sudden velocity breaks in the sonic log and with structural and petrographic variations revealed by the core evaluation. At 290 m depth, a strong reflection corresponds to a cataclastic shear zone which is interpreted as a late-Hercynian extensional fault zone. It is probably connected to a similar zone outcropping about 500 m north of the borehole.

3.4.3 Haslach "bright spot". An isolated reflection event beneath Haslach at about 9.5 km depth, which looks like a bright spot (Sheriff and Geldart, 1983), is located beneath the crossing area of three profiles near Haslach (cf. Fig. 12). Therefore, good three-dimensional control exists for stacked and migrated sections. They are presented in Fig. 18, together with a position map indicating the lateral extent of 3–5 km. The reflection amplitudes observed in true-amplitude sections are comparable to those of prominent reflections from the lower crust.

In view of the strong reflections from the bright spot, even in single-fold seismograms (source-point gathers), we tried to determine the polarity of the reflection coefficient. Single-fold uncorrected seismograms from source-point gathers were plotted in wiggle-area mode in two ways. Positive and negative values, respectively, above a certain threshold value were blackened and then compared to each other (Fig. 19). In traces with a high signal/noise ratio we may visually identify a symmetrical form of a Klauder wavelet consisting of a main lobe and two side lobes. This waveform represents a negative polarity of the reflection. The inspection of a variety of source-point gathers shows that wherever a Klauder wavelet can be recognized, its polarity is negative. This observation indicates that if the reflection is from a single interface, then it is caused by material of lower impedance than the surrounding medium. A velocity of 5.4–5.5 km/s of the surrounding medium is obtained from wide-angle experiments (see Sect. 4.1). Therefore, a velocity clearly below 5.4 km/s must be associated with material causing high-amplitude reflections with negative polarity. A possible explanation might be a concentration of trapped fluid. Its origin could be related to dehydration of Hercynian-age overthrusting of "wet" sediments. A similar bright spot appears on section 8514 (location 1350, 5 s TWT, cf. Fig. 14). The strong reflection amplitudes could result from contact between impervious rocks

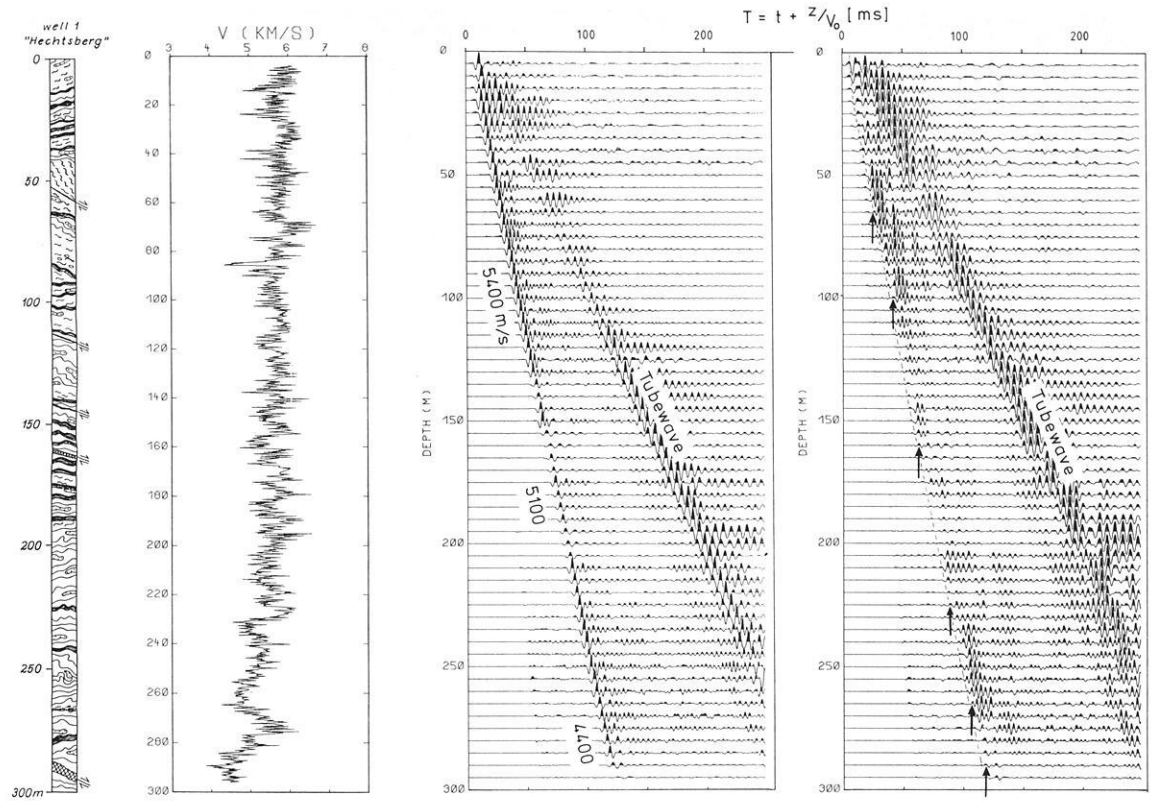

Fig. 17. Borehole data of "Hechtsberg" site. From left to right: – Structures and lithology derived from cores (simplified). Different gneisses and shear zones indicated. – Sonic log (digitized from analog data of Vogelsang, 1986). – Vertical seismic profiling (original data, vertical component). Clearly recognizable is the direct wave (labelled by corresponding velocities) and the tube wave. Note modified time scale. – Upgoing wavefield after application of a *f-k* filter. Note strong reflections, particularly from a cataclastic shear zone (depth 280 m). *Arrows* indicate reflections

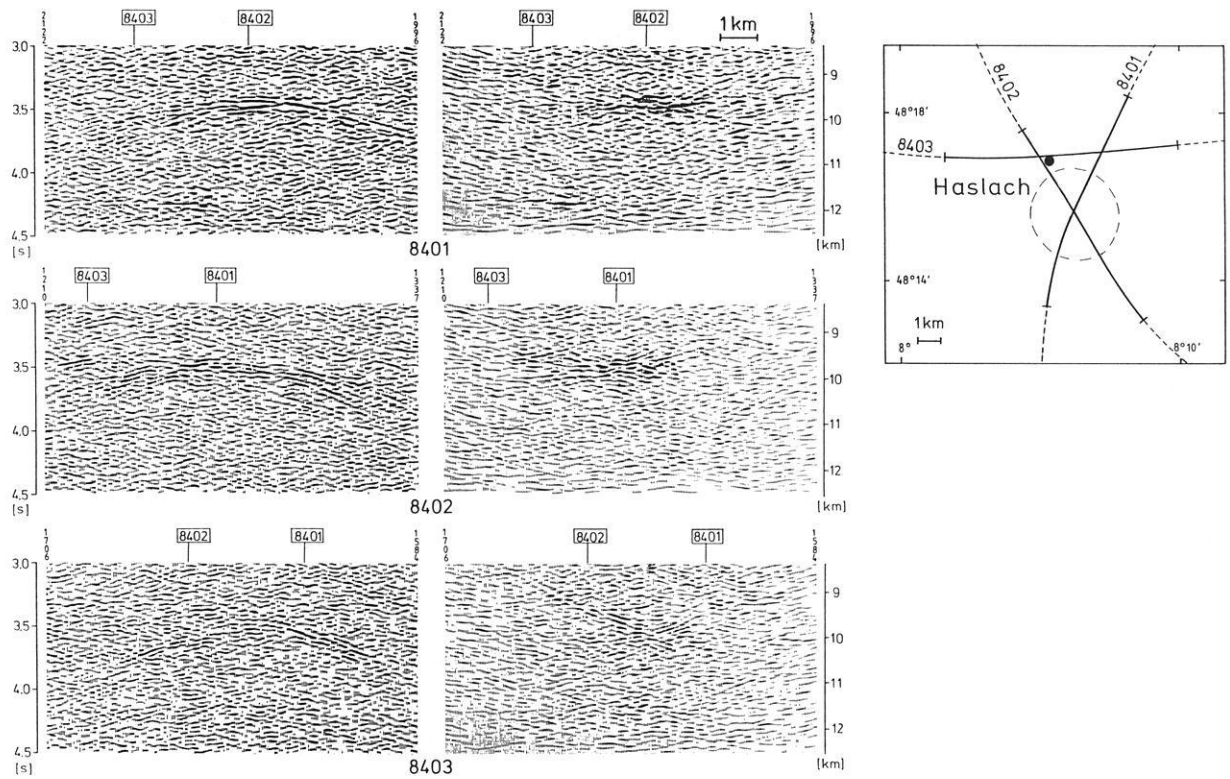

Fig. 18. Haslach "bright spot" represented by stacked (*left*) and migrated sections (*right*) of profiles 8401, 8402, 8403. Migration velocity 5700 m/s. Position sketch shows location and extent of the high-amplitude event (*dashed oval*). *Point* marks Haslach village

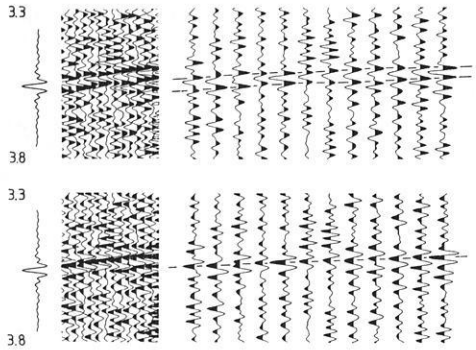

Fig. 19. Single-fold seismograms (line 8402) of the Haslach "bright spot" between 3.3 and 3.8 s TWT. Twelve traces are plotted with different spacings. In the *upper part*, the positive values are blackened; in the *lower part*, the negative ones. The theoretical Klauder wavelet with negative polarity is shown on the *left-hand side*. Positive values correspond to compression at the surface. The signals exhibit negative polarity because maximum correlation appears to the left

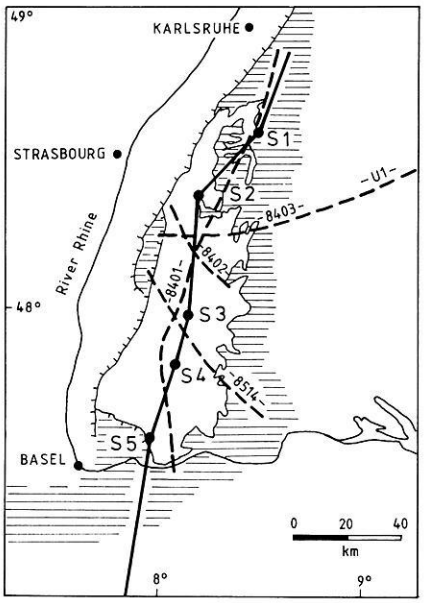

Fig. 20. Location map showing reflection profiles and the NS refraction profile. *Black circles* are shotpoints observed to both sides with receiver spacings of 1.5–2.0 km (from Gajewski and Prodehl, 1987)

and rocks with fluid-filled porosity. Lower crust or mantle-derived gases (CO_2, H_2O) may be trapped in addition to, or alternatively to, fluids from underthrusted sediments.

Similar bright spots were found in recent COCORP surveys (Brown et al., 1986). They are typically at midcrustal levels and can be of variable origin. Morton and Sleep (1985) inferred a magma chamber beneath an actively spreading back-arc basin from similar phenomena.

4 Velocity control by refraction and wide-angle reflection measurements

Whereas near-vertical reflection profiling provides detailed images of crustal structure, the reliability of the resulting velocity information is usually poor. For instance, the analysis of stacking velocities alone gives no hint of a low-velocity zone in the middle crust. Therefore, additional wide-angle measurements are required to determine the velocity needed for time-depth conversion and petrological interpretations. A gross two-dimensional velocity distribution was derived from refraction profiles. Expanding-spread soundings, focussed on the potential drilling site, were performed to deliver a high-precision velocity-depth distribution. In addition, a wide-angle Vibroseis experiment undershooting the Rhinegraben yielded velocity control for the adjacent graben proper and served to prepare a feasibility study for the Rhinegraben experiment in 1988 (Damotte et al., 1987).

4.1 Refraction profile

In August 1984 the Black Forest was studied by a seismic refraction survey along a 240-km NS profile from its northern end to the Swiss Molasse Basin (Gajewski and Prodehl, 1987; Fig. 20). Five shots, offset by 30–40 km, were recorded with stations spaced between 1.5 and 2 km apart. The geometry was designed to resolve a two-dimensional velocity distribution. The velocity model, displayed in Fig. 32, is essentially based on the correlation of the P_G wave diving through the uppermost crust, reflections P_L from the top of the lower crust and P_M from the crust-mantle boundary. The model was successively improved by synthetic seismograms based on two-dimensional asymptotic ray theory (Gajewski and Prodehl, 1987).

The main finding is a low-velocity zone (5.4–5.5 km/s) which is pronounced in the northern and central Black Forest and which fades out to the south. It is located directly on top of the lower crust which has an average velocity of 6.6 km/s. The top of the lower crust is at a depth of 14–15 km beneath the central Black Forest. In this model the crust-mantle boundary appears as a first-order discontinuity and does not show any major depth variations north of the Swiss Molasse Basin.

The refraction line and the NS reflection profile 8401 practically coincide. Structural features observed in near-vertical reflection sections and velocity information inferred from wide-angle measurements were jointly evaluated.

4.2 Expanding-spread profile

From the results of the refraction and reflection profiles, the region around Haslach appeared as typical normal Moldanubian crust right in the centre between two large thrust zones (Baden-Baden zone in the north and Badenweiler-Lenzkirch zone in the south). It was therefore decided to explore this crustal section and its velocity structure by an expanding-spread profile (ESP). The principal goals of this experiment were:

1) To investigate the nature of the bright spot at about 9.5 km depth (see Sect. 3.4.3).

2) To determine the average velocities in the upper crust and the entire crust for precise time-depth conversions.

3) To investigate the wide-angle characteristics of the lamellar lower-crustal reflections.

Our intention was to get high-resolution observations in the wide-angle range, comparable to the resolution of the near-vertical recordings. Small explosive charges of 10–50 kg were used as sources, distributed in patterns of 30–50 shallow drillholes (depth 2–3 m) in crystalline rock.

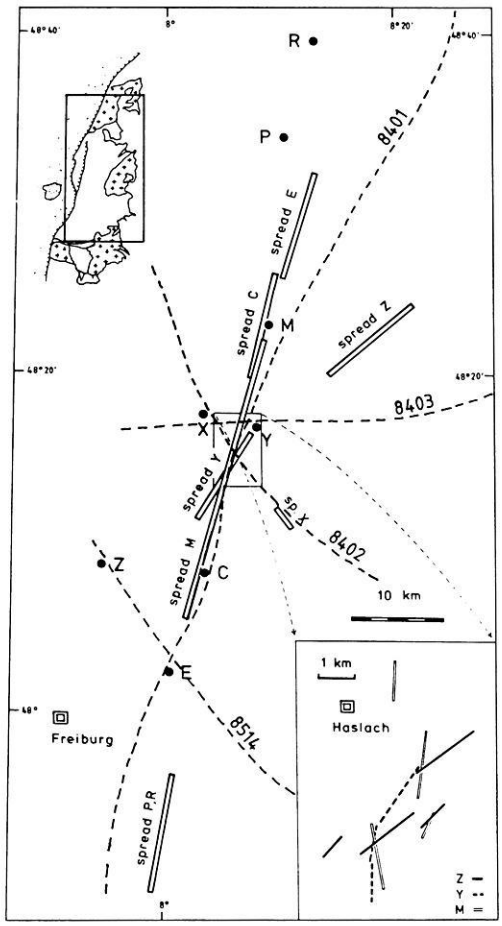

Fig. 21. Schematic map of the "expanding-spread" profile with shotpoints and corresponding geophone layouts consisting of four independent digital recording units. The *inset* shows the blown-up central region with true midpoint configurations for shots *M*, *Y* and *Z* covering the lateral extent of the Haslach "bright spot". The map also shows the location of reflection profiles

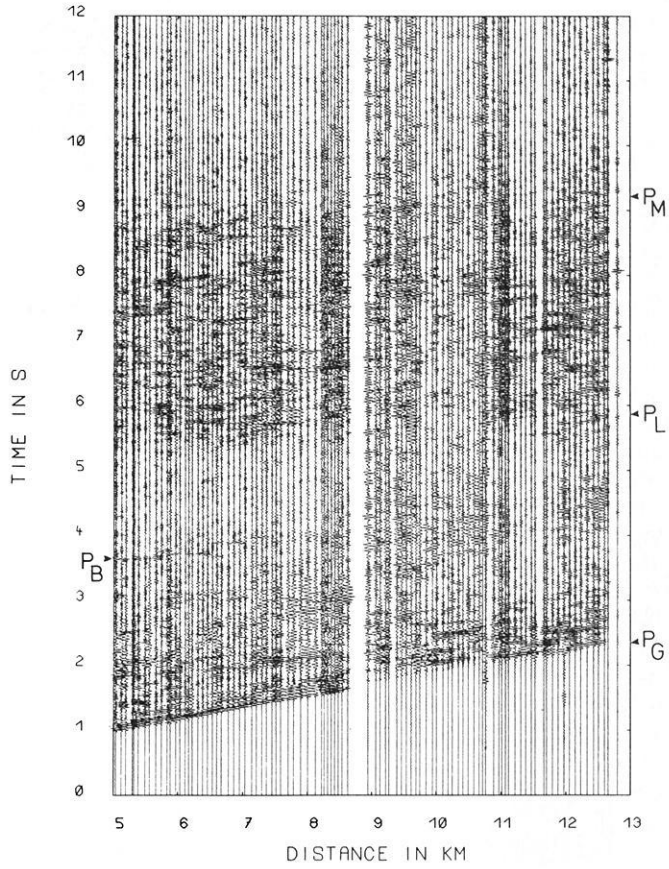

Fig. 22. Section of shotpoint *Y* observed by three multichannel digital recording units in the offset range 5–13 km. Time scale is unreduced. P_G – first arrivals from crystalline diving wave, followed by upper-crustal reflections of local character. P_B – bright spot phase. These signals are missing at greater offsets (cf. Fig. 23). P_L – first of lower-crustal reflections. P_M – latest reflections which correlate with the Moho phase from refraction survey and from modelling. Amplitudes are normalized for each trace

This arrangement produced a broadband signal with dominant frequencies between 20 and 30 Hz. Shot R in the north (Fig. 21) was fired in a similar arrangement and with 60-kg charge in a small pond. The recording spread consisted of 144 channels spaced 80 m apart, enabling exact phase correlation; whereas in the refraction experiment (Sect. 4.1), a spacing of 1.5–2.0 km was used.

The field experiment was performed in October 1985. The locations and corresponding geophone spreads, together with common midpoint ranges of some selected recordings (shots M, Y and Z), are given in Fig. 21. In total, eight different shotpoints were chosen for data evaluation. The recordings from shotpoints Y and Z are shown in Figs. 22 and 23. In both seismogram sections a clear P_G phase from the first arrivals can be identified. Phases reflected from the bright spot at about 9.5 km depth (phase P_B) can only be correlated in the record section of shot Y in the near-vertical range. It is followed by a band of strong reflections from the laminated lower crust, beginning with phase P_L caused by the same laminated structure seen in near-vertical sections. With the small geophone spacing of 80 m, it is possible to correlate individual phases over 400–1500 m. Consequently, the lateral extent of single lamellae is of the order of 200–800 m (see also Sect. 5.2). By contrast, in the refraction profile with a geophone spacing of 1.5–2.0 km, these small-scale reflecting structures cannot be resolved. Therefore, a correlation in widely spaced refraction measurements is subject to spatial aliasing simulating large-scale structures.

From the geometric configuration of the expanding-spread profile, the average velocity down to the first lamellae of the lower crust is determined using the T^2–X^2 diagram for the combined sections of shots M, Y and Z (Fig. 24). The slope of the solid straight line fitting the beginning of lower-crustal reflections yields an average velocity of 5.62 km/s. The error bounds are not more than $\pm 2\%$, taking vertical two-way travel times and travel times of reflections at individual common midpoints from the original data set into account. The sensitivity of this procedure is demonstrated by the dashed lines in Fig. 24, corresponding to a velocity increase of 0.1 and 0.2 km/s. This approach is only valid for a homogeneous medium. In a stratified medium this is an approximate procedure, and velocity and depth do not necessarily coincide with the true RMS values. For the upper crust we studied the possible variations by comparing the true and the apparent RMS velocities for a variety of realistic models. We never found deviations larger than 0.02 km/s. The average velocity of 5.62 km/s $\pm$

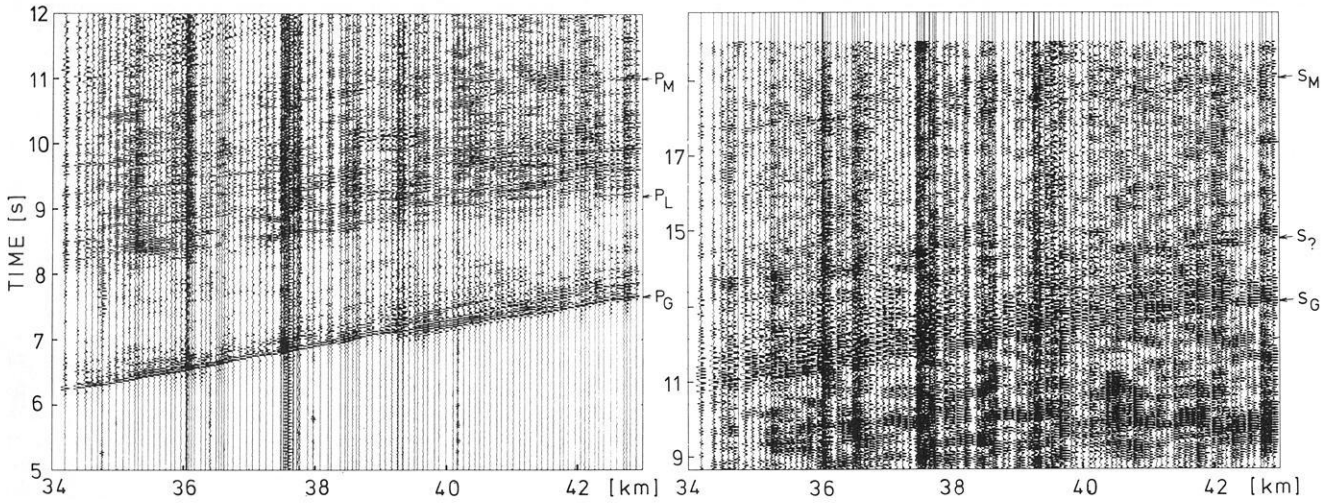

Fig. 23. Section from shotpoint *Z* with offset range 34–43 km. The *left part* shows compressional-wave arrivals P_G, P_L, P_M (cf. Fig. 22). The *right part* is from the same recording with a time scale multiplied by $\sqrt{3}$. Coherent phases can be compared with corresponding *P* phases. S_G and S_M are clearly identified as shear waves. The $S_?$ phase can be alternatively interpreted as S_L or as a converted phase (S_MP) from the crust-mantle boundary

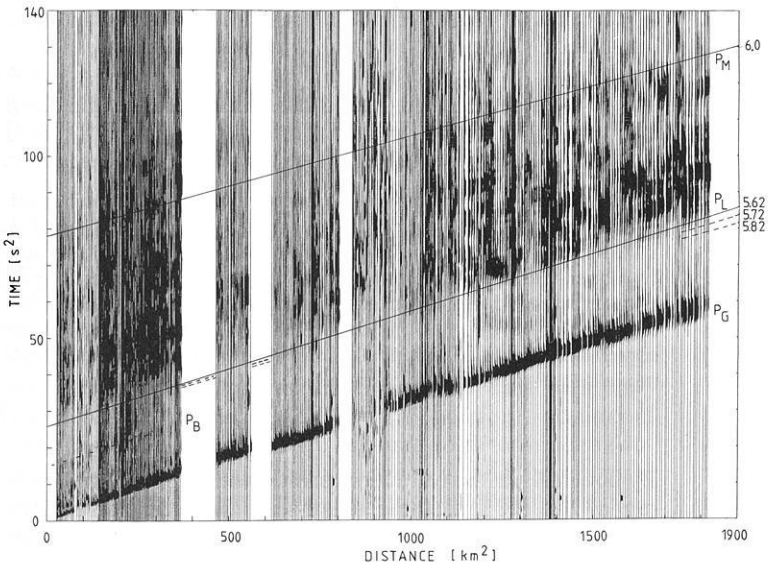

Fig. 24. T^2–X^2 presentation of expanding-spread data for shots *M*, *Y*, *Z* and corresponding spreads arranged according to distance from shotpoints within 0–43 km offset range. The seismograms are displayed as energy traces. *Solid straight lines* yield RMS velocities (values in km/s at the *right-hand side*) for the upper crust and for the whole crust, respectively. They are determined by the vertical TWT, i.e. t_o, fixed by the near-vertical reflection profiles within ± 0.2 s for the whole Haslach region and by the first and last reflected energy from the lower crust in this diagram. The sensitivity of this procedure is indicated by *dashed lines* with greater values and fixed time t_o

2% for the upper crust confirms the results of modelling the refraction data (Sect. 5.1), especially the reality of the low-velocity zone between 7 and 14 km depth.

The average velocity down to the crust-mantle boundary defined by the last reflected energy corresponding to phase P_M is estimated to be 6.0 km/s $\pm$ 4%, giving an interval velocity of about 6.5 km/s for the lower crust in agreement with the refraction modelling (Sect. 5).

In the ESP sections, shear-wave phases from the upper crust and the crust-mantle boundary can be correlated and compared with the corresponding *P* phases in the undercritical as well as in the supercritical range. Two seismogram sections for different distance ranges have been subdivided into a *P*- and a *S*-wave section in Figs. 23 and 25. The time-scale of the *S*-wave section is amplified by $\sqrt{3}$, corresponding to a Poisson's ratio of 0.25. In Fig. 23 the *P*-wave section shows the characteristic response of the crust in the upper (P_G phase) and lower part (phase P_L and P_M characterizing top and bottom of the laminated lower crust). In the *S* wave section, the diving wave from the upper crust (S_G) has the same velocity in the amplified time scale as the corresponding *P* phase. Therefore, Poisson's ratio is normal in the penetrated part of the upper crust. A distinct onset from the Moho (S_M) can also be correlated, yielding the same Poisson's ratio for the whole crust; whereas the lower crustal *S*-wave reflections cannot be identified unequivocally. The phase $S_?$ can be interpreted in two ways:

A) It represents the converted $P-S$ phase from the Moho.

B) It characterizes the *S*-wave reflection from the top of the lower crust, which would imply a strong reduction of Poisson's ratio in the low-velocity zone in order to explain the time-shift with respect to the *P*-wave reflection.

A similar comparison at supercritical offsets shows the same results in this range (Fig. 25). In contrast to the situation in the undercritical range, the travel time differences between converted $P-S$ phases from the Moho and the shear-wave reflections from the top of the lower crust are

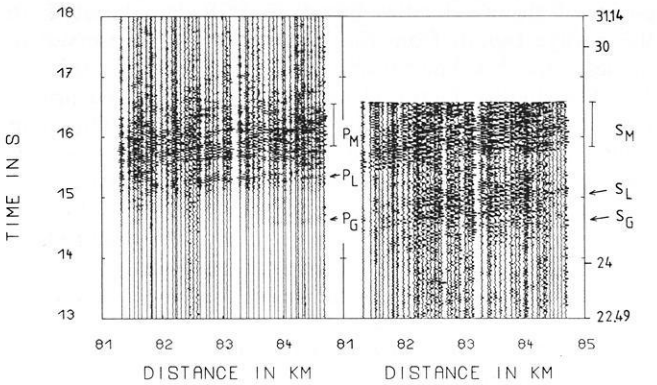

Fig. 25. Section from shotpoint *R* with a selected offset range of 81–85 km. *P* waves on the *left*, *S* waves on the *right*. The *right-hand part* is from the same recording with a time scale multiplied by $\sqrt{3}$. Coherent phases can be compared with corresponding *P* phases. S_L arrivals are faster than P_L with respect to a ratio of 1.73. This indicates that the mean value of the V_p/V_s ratio (or Poisson's ratio) for the upper crust is less than 1.73

large enough to allow for the unequivocal identification of the S_L phase. P_L and S_L exhibit a significant time difference with an average V_p/V_s ratio of only 1.67 down to the top of the lower crust. With respect to this low mean value, the velocity ratio in the *P*-wave low-velocity zone must be further reduced regarding the value 1.73 in the first 6–7 km depth obtained from shotpoint Z. For the whole crust, a V_p/V_s ratio of 1.73 as a mean value is inferred from P_M and S_M phases. In order to compensate for the reduction within the *P*-wave low-velocity zone, an increase of the V_p/V_s ratio in the lower crust must be assumed. These observations are based on shotpoints Z (Fig. 23), P and R (Fig. 25). The other shotpoints did not generate enough shear-wave energy to provide reliable correlations on vertical-component recordings. These qualitative results need further justification by a controlled shear-wave experiment scheduled for 1987.

During the KTB reflection campaign, a wide-angle Vibroseis experiment was carried out as a joint ECORS/DEKORP operation as a feasibility study concerning a future seismic reflection survey of the Rhinegraben rift. Details concerning data acquisition, communication, data processing and influence of near-surface geology are given in Damotte et al. (1987). In Fig. 26 the data of this Rhinegraben undershooting test are compared with expanding-spread records of the Black Forest in the offset range 70–85 km. The *P* arrivals of the lower crust beneath the Rhinegraben are about 0.3 s later than from beneath the Black Forest, both phases being propagated on a purely crystalline path. The duration of the lower-crustal reverberations amounts to about 1 s in the Rhinegraben compared to 2 s in the Black Forest, indicating a thickness ratio of about 1:2 in the lower crust. These observations agree very well with the reflection-seismic findings of Dohr (1970). In his section obtained in the central graben near Rastatt, south of Karlsruhe, the difference in TWT between the top of the lamellae at about 7 s and the bottom of the sedimentary fill near 2 s is just 5 s; as is the TWT through the crystalline basement from the surface to the top of the lamellae in this KTB reflection data in the Black Forest. One possible interpretation is that the entire brittle upper crust of the graben subsided without appreciable change in thickness during Tertiary graben formation. A comprehensive discussion of consequences of this hypothesis for crustal development can be found in Fuchs et al. (1987).

Probably the most outstanding feature is the different energy distribution in Fig. 26. In the Black Forest the greatest amplitudes come from lamellae near the crust-mantle

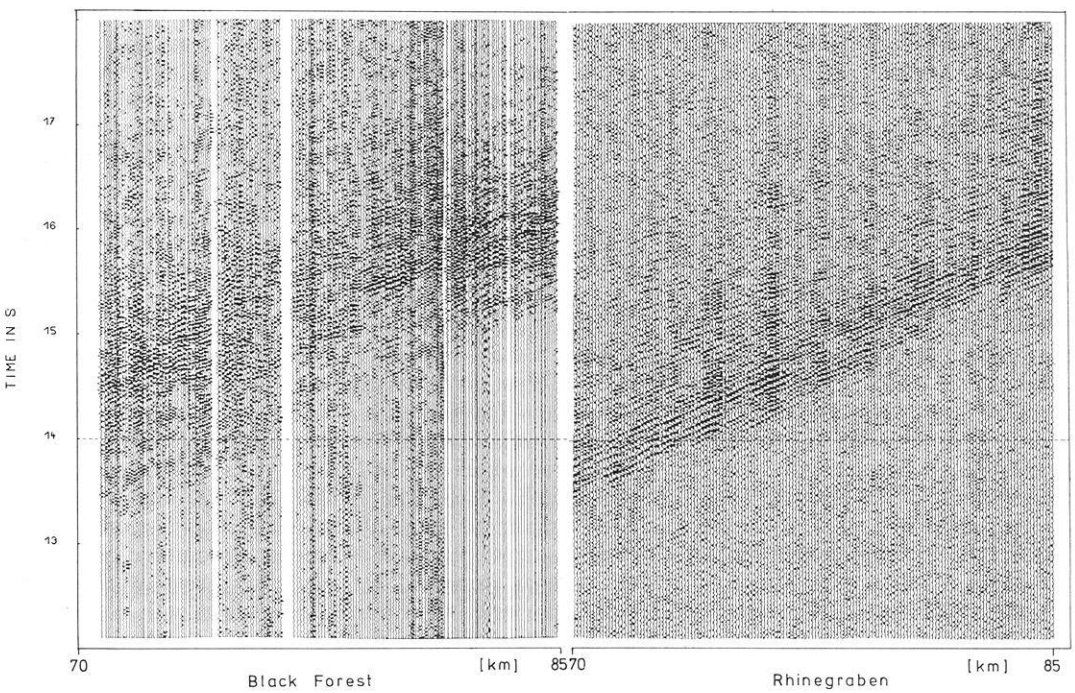

Fig. 26. Comparison of wide-angle seismograms from the expanding-spread profile in the Black Forest (*left panel;* shots *R*, *P* and corresponding spreads) and the Rhinegraben undershooting (*right panel;* vibrators in the Black Forest, recording spread in the Vosges Mountains of WE profile at 48°15′ latitude). Time scales not reduced

boundary, whereas in the Rhinegraben most of the energy is concentrated in the earlier reflections from the lower crust. This indicates stronger velocity contrasts of the upper part of the lower crust in the Rhinegraben than beneath the Black Forest.

5 Seismic modelling

Important constraints on the physical properties of the earth's crust are provided by determining compressional and shear wave velocities from refraction seismic data. Gajewski and Prodehl (1987) derived a two-dimensional model by ray-tracing methods and asymptotic ray theory (see Sect. 4.1). Here we focus on the central Black Forest, modelling the record section of shotpoint S3 (Figs. 20 and 27) by the reflectivity method (RM) of Fuchs and Mueller (1971). Several circumstances are favourable in this respect. The shot was detonated in crystalline basement rocks and generated a broadband source signal with frequencies up to 25 Hz. In the two-dimensional velocity model of Gajewski and Prodehl (1987) and in the structural image of the Vibroseis survey, the crustal region north of S3 appears to be sufficiently laterally homogeneous that the RM can be applied. The computations are performed on a CDC CYBER 205 so extremely fast that we do not face any practical limits concerning vertical complexity, frequency content and number of models (Sandmeier and Wenzel, 1986). Since reflection profile 8401 almost coincides with the refraction line, we can compare results of two-dimensional modelling of source-point gathers with those of the RM.

The interpretation of refraction and reflection data sets of the same region with different sophisticated modelling techniques yields a detailed image of the crustal velocity structure of the central Black Forest.

5.1 Modelling of wide-angle seismograms

As the modelling procedure has been described in detail in Sandmeier and Wenzel (1986), the results are only summarized here. An attempt was made to match not only particular phases such as those from the upper and lower crust (P_G, P_L), the Moho reflection (P_M), and shear-wave onsets, but the entire wavefield in the observational parameter space of offset and travel time. We do not consider the data set to be composed of several distinct phases and some kind of noise; but, rather, we realize that the long reverberations are mainly caused by the lamination of the lower crust and that their amplitude and frequency behaviour reflects properties of the lamination. This point of view turns out to be significant because the classic idea of phase correlation inherently contains a high-frequency approximation and breaks down if it is applied to a structure layered on a scale less than a dominant wavelength. However, this is the case in the lower crust of the central Black Forest. We elaborate this point further in Sect. 6. In order to find error bounds for our model, the parameter space consisting of compressional and shear velocity and attenuation as functions of depth was systematically sampled. About 60 different models were calculated for this purpose.

Figure 27 shows the data of shotpoint S3, the best model we found and the corresponding synthetic seismogram section. The ratio of compressional to shear velocities is assumed to be $1/\sqrt{3}$. This value does not contradict the interpretation of shear velocities based on ESP data because no shear-wave signals from the lower crust were observed in the section of S3. The density is given by $\rho = 0.252 + 0.3788 \cdot V_P$. The quality factor Q amounts to 400 in the upper, 1000 in the middle and 2000 in the lower crust. The main results can be summarized as follows. There is a pronounced low-velocity channel in the upper crust with a reduction in seismic velocity from 6.0 to 5.5 km/s. It is located directly above the laminated lower crust. The thickness of the lamellae is randomly varied with an average value of 120 ± 30 m. The average local velocity in the lower crust increases from 6.0 to 6.8 km/s. The magnitude of the reflection coefficients increases from top to bottom. The crust-mantle boundary is modelled as a step-like transition zone consisting of first-order discontinuities. The mean V_p/V_s ratio has been proved to be normal.

In Fig. 28 [panels (b)–(f)] synthetic seismograms for 5 out of about 60 models are presented in order to give an impression of the sensitivity of the synthetics in reaction to model variations. Panel (a) displays the data at offsets between 50 and 80 km reduced with 8 km/s. The main phases labelled P_G, P_L, P_M in Fig. 27 are clearly recognizable in this range. In (b) the synthetic seismograms of the best solution are displayed. In (c) the average thickness of the lamellae is increased to 200 m instead of 120 m. The reverberations from the lower crust change significantly. They are small at small offsets and become larger beyond 75 km, and the amplitudes around 70 km grow compared to those of the Moho reflection. A similar obvious misfit with the data appears if the average thickness is decreased to 50 m [panel (d)]. The amplitudes of the P_L wavetrain become much smaller relative to P_G and they almost disappear between 65 and 75 km. In the model of Fig. 27, the lamellae ride on a gradient structure of 0.21 s^{-1} between 15 and 18.5 km and 0.07 s^{-1} between 18.5 and 23.5 km depth. The variation of the gradient is not arbitrary. If it is replaced by a constant gradient, the P_L reverberations get only gradually weaker between 60 and 75 km as panel (e) demonstrates; whereas the double gradient results in a sharper drop in amplitude at 65 km, in agreement with the observation [cf. panel (a)]. An evidently unsatisfactory synthetic record section arises if the gradient is assumed to be zero, so that the lamellae are simply superimposed on a constant velocity of 6.7 km/s [panel (f)].

In order to test the significance of the frequency content for modelling a complex structure, we have applied a 15-cps low-pass filter (Fig. 29) to the particular seismogram sections of Fig. 28. In this case it is not possible to draw the same conclusions from modelling the data as in the high-frequency case. Apart from panel (f), the response from the lower crust is remarkably diminished and from the real data of panel (a) we would not expect a laminated structure with high reflectivity above the crust-mantle boundary. It is not clear which model fits the data best, although the characteristics described above for the high-frequency source remain the same qualitatively. This example shows that physical properties of a complex structure (e.g. a laminated zone as proposed for the lower crust of the Black Forest) can only be inferred from data with sufficiently high frequencies. As in most of the earlier refraction profiles, low frequencies around 10 Hz are dominant; their interpretation generally cannot reveal the complexity of the crust, but represents only an average over the prevailing wavelength.

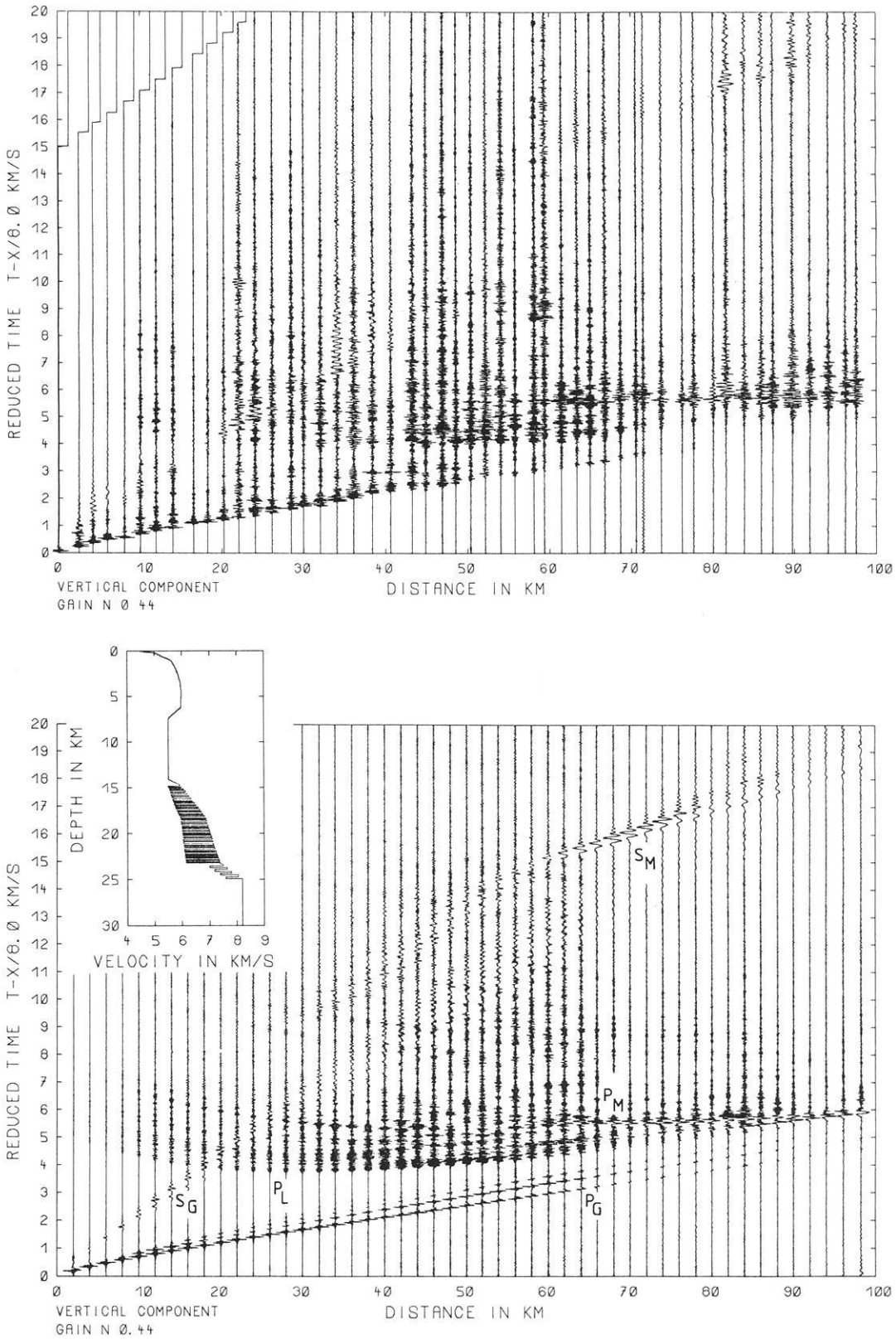

Fig. 27. Reflectivity-modelling of the refraction profile S3-North. Observed data in the *upper part*, synthetic seismograms in the *lower part* (time scale reduced with 8 km/s). *Inset* shows corresponding velocity-depth function. The splitting of P_G phases is due to surface multiples

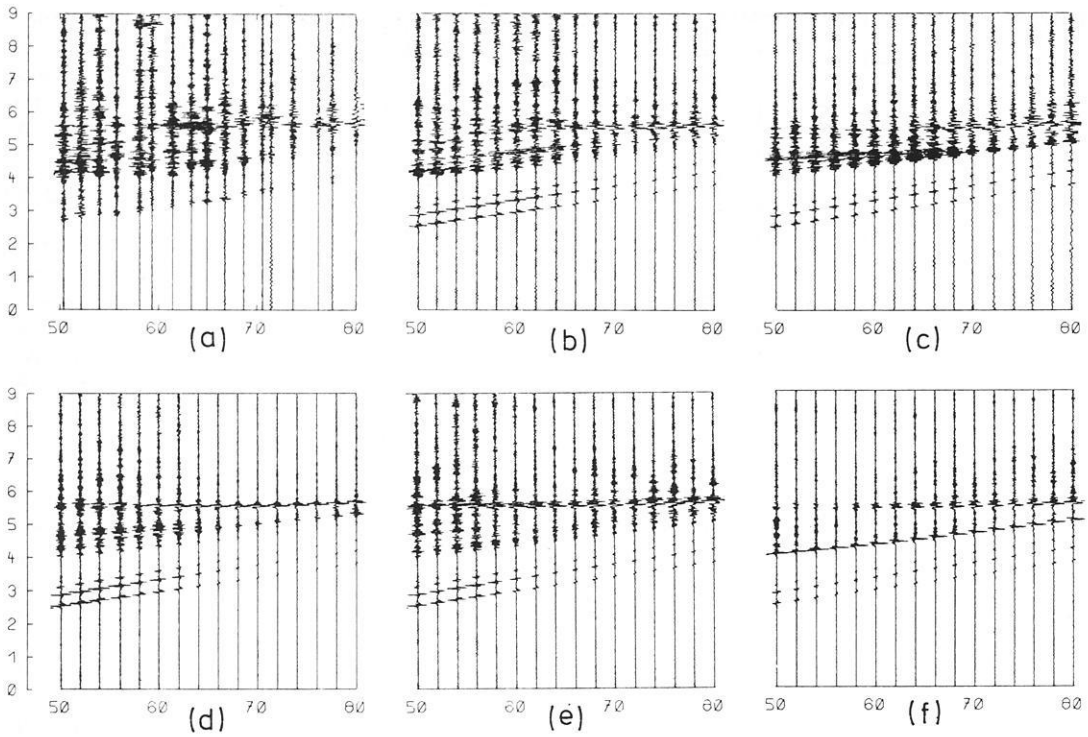

Fig. 28. Synthetic seismogram sections for offset range 50–80 km: (*a*) observed data (same as in Fig. 27 upper part); (*b*) synthetic data of final model (same as in Fig. 27 lower part), average lamellae thickness 120 m; (*c*) synthetic data corresponding to modified model with lamellae of average thickness of 200 m; (*d*) thickness of lamellae = 50 m; (*e*) single lower-crustal velocity gradient instead of two gradients; (*f*) no gradient superimposed on lamellae. Average crustal velocities are the same in (b)–(f)

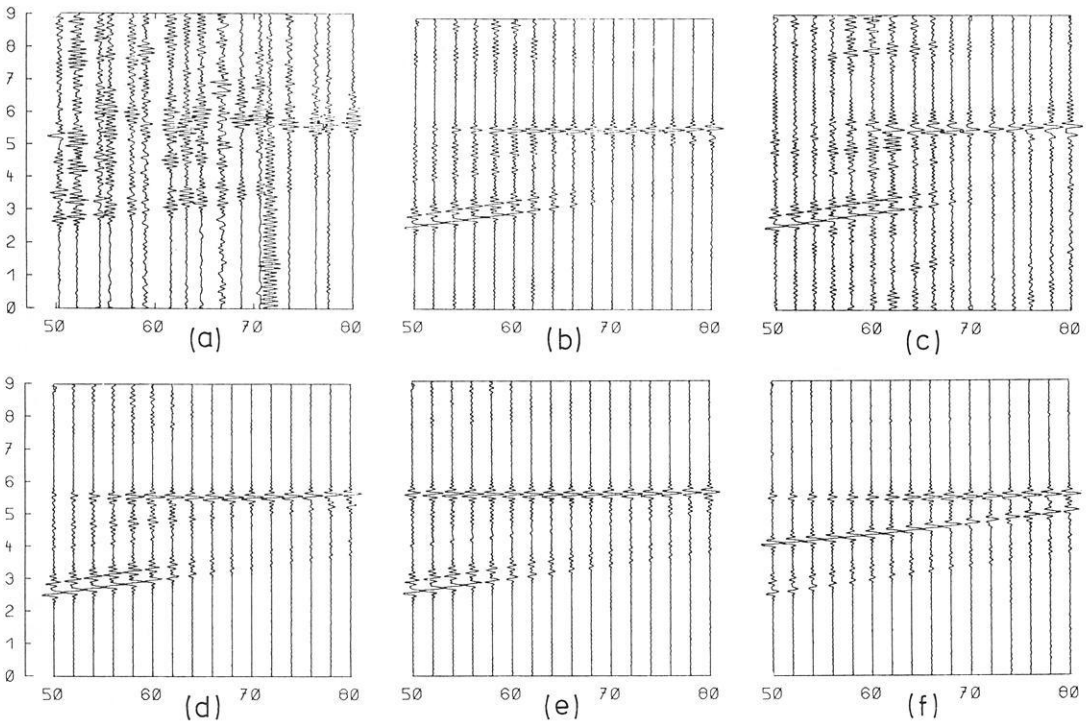

Fig. 29. Observed and synthetic seismograms corresponding to the same models as in Fig. 28, but low-pass filtered with 15 Hz cut-off. Note that lower-crustal reverberations are not clearly recognizable

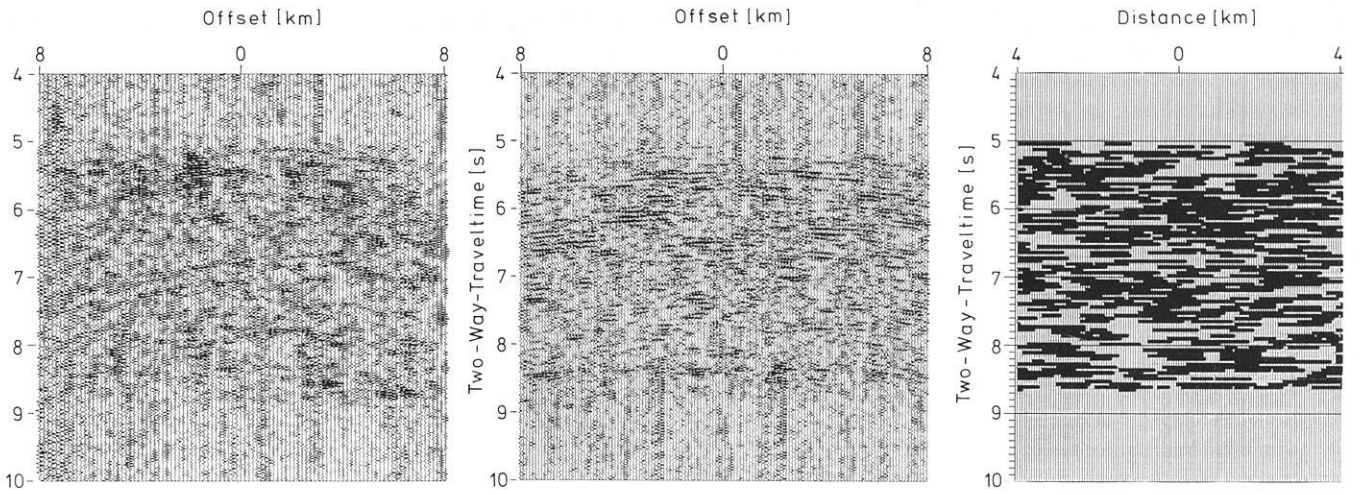

Fig. 30. Two-dimensional modelling of a common vibrator-point gather. Observed data are shown in the *left-hand panel* from 4 to 10 s TWT. Synthetic seismograms are displayed in the *central panel*; the corresponding model in the *right-hand panel. Dark areas* represent high-velocity lamellae imbedded in a lower back-ground velocity. Special emphasis was placed on the lamellar structure of the lower crust. The lamella distribution with depth is varied laterally. Lamellae have randomly distributed horizontal extents of 1–2 km. See text for further explanations

5.2 Modelling of near-vertical seismograms

A shortcoming of the RM is that the medium has to be laterally homogeneous. Despite the fact that velocities in the central Black Forest are only slowly varying laterally, we know from reflection sections that the lower crust contains numerous reflecting elements with apparent lengths in the kilometre range and that it is therefore laterally variable on this scale. We focussed our interest on two problems: (1) What kind of two-dimensional structure has to be assumed to provide reflection seismograms as observed in the central Black Forest? (2) How do those models compare with the one-dimensional model derived with the RM? For this purpose we employed a program that solves the two-dimensional acoustic wave equation numerically (Wenzel et al., 1987). It follows the approach of Gazdag (1981) and Kosloff and Baysal (1982) who calculate the spatial derivatives in the wave equation with Fourier transform methods. With this algorithm, which is implemented on the CDC CYBER 205, the seismic response of a crustal block of 30×30 km^2, a size large enough to synthesize source-point gathers, can be calculated. Steep travel paths of lower-crustal reflections are assumed in order to prevent conversion so that the equations of elasticity degenerate into acoustic equations. On the other hand, full wave solutions are required because the fact that the lower crust apparently contains many features in the range of a wavelength or less prohibits high-frequency approximations.

The utilisation of the two-dimensional acoustic wave equation does not allow a quantitative comparison of synthetic seismograms and data because a line source is assumed instead of a point source, and only velocity variations (i.e. compressibility variations) are considered while density remains constant. However, a qualitative comparison based on the abundance of reflection events, their lateral extent and consistence is possible.

The lower crust is modelled with randomly distributed lamellae of variable length, thickness and concentration. A single lamella is generated by imbedding a high-velocity rectangle within a lower background velocity. Figure 30 shows an observed source-point gather and a synthetic one containing only lower-crustal reflections. Here we used lamellae with a thickness of 120 m and lengths between 1 and 2 km. The number of high-velocity lamellae is such that the total area filled with lower-velocity material equals the area with higher values. If we deviate significantly from this selection of parameters, the overall appearance of the synthetics loses its similarity with the data in the sense that reflections become laterally too consistent or too numerous. The wavelet is a sweep autocorrelation function with frequencies between 10 and 35 Hz. The data have been filtered with the same frequency window to allow comparison. Details of the numerical method and of the results are given in Wenzel et al., (1987). Here we only present one example of the results: a structure containing randomly distributed lamellae shows a reflection response with characteristics similar to the data if the parameters mentioned before are used. Along vertical cross-sections through the two-dimensional model we get sequences of alternating high- and low-velocity layers with an average thickness of 120 m. This is in agreement with the result derived by modelling of refraction data with the RM.

6 Compilation of velocity information

Following our concept of unified interpretation of all accessible data, we analyse observed and modelled velocities in terms of their compatibility. Figure 31 shows the available velocity information derived for the central Black Forest near Haslach. Physical velocities are displayed as local and root-mean-square values (RMS), respectively. Solid lines represent these compressional-wave velocities inferred from modelling of refraction seismograms with the reflectivity method (RM). Dashed lines correspond to refraction interpretations of the same record section based on asymptotic ray theory (ART). For details, see Sects. 4.1 and 5. Dotted lines represent stacking velocities used for processing the data of reflection profiles 8401, 8402, 8403 near Haslach.

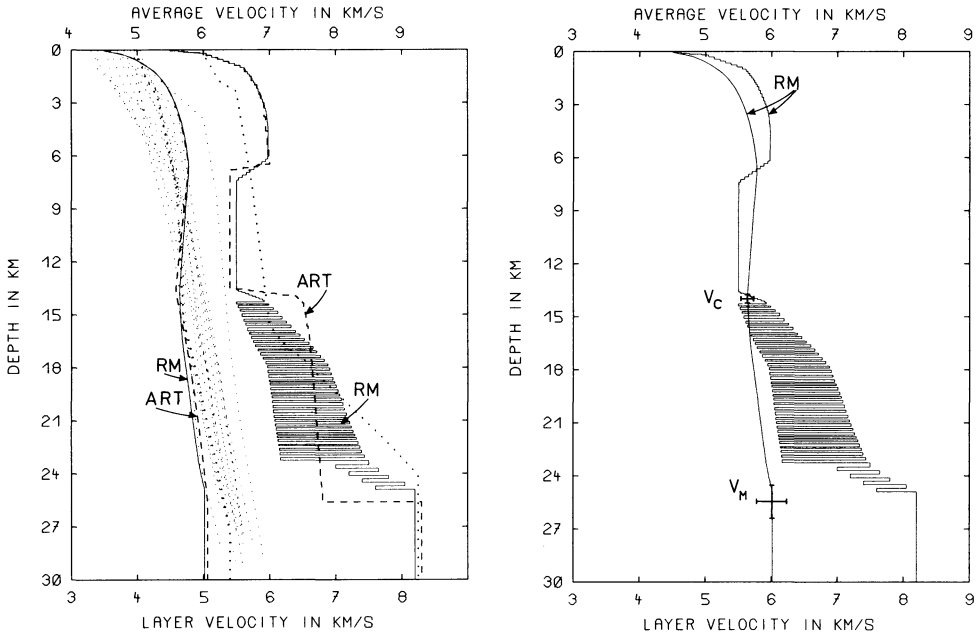

Fig. 31. Velocity compilation for the central Black Forest (near Haslach). *Left panel:* local velocities from ray-tracing (ART) and reflectivity (RM) modelling (*dashed and solid lines*, respectively; scale at the *bottom*). Corresponding RMS velocities are displaced by one unit to the left (scale on *top*; *dashed and solid lines*) together with stacking velocities of the reflection survey (*dotted lines*). *Thick dots* represent interval velocities derived from a typical stacking velocity function. *Right panel:* comparison of RMS velocities of the final RM model and ESP-derived values of $V_C = 5.62$ km/s $\pm 2\%$ for the upper crust and of $V_M = 6$ km/s $\pm 4\%$ for the entire crust (cf. Fig. 24). Corresponding depth uncertainties are $\pm 2\%$ and $\pm 4\%$, respectively. For completeness, the interval velocities of the RM model are shown at the same scale

Physical velocities. Two velocity-depth functions were independently derived from the 1984 refraction experiment using RM and ART for interpretation. Both models coincide in the upper 7 km and in the thickness of the low-velocity channel, where the velocities differ only slightly. Consequently, the position of the top of the lower crust is in agreement. A striking difference appears in the lower crust. For its upper part, a relatively high velocity (6.5 km/s) is derived by Gajewski and Prodehl (1987) from a phase correlated at the outermost parts of the profile and interpreted as a diving wave. This phase cannot be clearly recognized in the profile of shotpoint S3 displayed in Fig. 27 because of its restricted offset range. Better evidence is attained in the sections of adjacent shotpoints S2 and S4 which have a larger offset. The details of the lower-crustal RM model are essentially constrained by the data in the offset range between 40 and 90 km. Our RM model does not reproduce the diving wave from the lower crust. It could only be generated in the synthetic seismograms by increasing the velocities between 14 and 18 km depth to 6.5 km/s. However, in this case a much poorer fit of the data, in terms of amplitude and frequency characteristics in the offset range up to 90 km, would result. Consequently, we conclude that an interpretation of the record sections in the frame of a one-dimensional model is incomplete. The remaining discrepancies must be attributed to lateral variations of depth and magnitude of velocity contrasts.

Both interpretations of the data agree in the RMS velocities throughout the whole crust and in the depth of the crust-mantle boundary at about 25 km as a first-order discontinuity. The major features of the velocity-depth profile presented here are qualitatively in good agreement with previously derived models; see Mueller et al. (1969), Mueller (1977) and Deichmann and Ansorge (1983).

Stacking velocities. Representative stacking velocities for the central Black Forest are displayed as dotted lines in the left panel of Fig. 31. They show considerable variation within a range of 1 km/s at all depths. In order to examine their compatibility with refraction velocities, one has to be aware of their meaning and accuracy. Stacking velocities are formal velocities used to produce a stacked section with optimum contrasting structures; consequently, they must be considered processing velocities. In our case 20–50 CDPs were first stacked with trial velocities, then displayed and, finally, the best section was chosen by individual judgement. Under certain circumstances stacking velocities are closely related to physical velocities. If a horizontal reflector is overlain by a laterally homogeneous medium and if the recording offsets are within the hyperbolic range, the best stack should arise if the stacking velocity is the physical RMS velocity (Dix, 1955). The accuracy of its determination is limited however (Hajnal and Sereda, 1981). Dipping reflectors and point diffractors have optimum stacking velocities larger than the physical ones (Dinstel, 1971). As both events and diffractions are observed in the lower crust of the central Black Forest, we attribute the systematic deviation of the stacking velocity from the physical RMS value to these features. Similar observations are reported from the DEKORP 2-South reflection profile (Bortfeld et al., 1985). Further discrepancies are introduced if lateral velocity inhomogeneities along a CDP are present. These effects have been studied, e.g. by Miller (1974) and Blackburn (1980), with respect to sedimentary regions. However, in the crystalline environment of the Black Forest the physical velocities do not change dramatically. Another point is that CDPs very often do not show consistent reflectors in the crystalline basement. Therefore, an interpretation of stacking velocities of the type familiar from exploration

experience in sedimentary regions must be regarded with caution. If, however, the stacking process is focussed on a consistent reflection, e.g. from the Moho using a recording spread of more than 20 km, a reliable interpretation of stacking velocities in terms of physical velocities is possible. This has been demonstrated on the 1978 Urach reflection profile (Bartelsen et al., 1982).

The stacking velocities are biased towards low values in the upper crust and towards high values in the lower crust (left panel of Fig. 31). We cannot yet present a straightforward explanation of this fact.

Comparing stacking and refraction velocities we have to consider that the stacking velocity involves vertical ray paths and the refraction velocity mostly horizontal ray paths. Discrepancies could then be caused by seismic anisotropy (Winterstein, 1986).

7 Compilation of geophysical data and geological-petrological interpretation

7.1 Data

The deployment of a variety of geophysical sounding tools on a regional scale gives a synchronous view of crustal properties through different imaging techniques. Physical anomalies and gradients may be tested for their compatibility and consistency. In Fig. 32 structural information from the Vibroseis reflection profile 8401 (from Fig. 8), the refraction seismic model from Gajewski and Prodehl (1987), the Bouguer gravity anomaly along the seismic profile 8401 (Götze et al., 1986), the heat-flow distribution derived from borehole measurements (Stiefel et al., 1985) and the seismicity distribution (Bonjer and Apopei, personal communication) are displayed. Additional information obtained on electrical conductivity from magnetotelluric and electromagnetic sounding methods has been presented by Berktold et al. (1985) and by the LOTEM Working Group (1986).

One of the most exciting questions concerns the compatibility of crustal discontinuities defined by refraction and reflection methods, i.e. the compatibility of wide-angle and near-vertical measurements. Wide-angle refraction ray paths are sensitive to large-scale vertical and horizontal velocity gradients. Near-vertical incidence of elastic waves more accurately images the vertical sequences of fine structures, in terms of their reflectivity, at a resolution within the scale of the seismic wavelength. Gajewski and Prodehl (1987) transformed their refraction velocity-depth model to a velocity–vertical–travel-time (TWT) model and compared it to the near-vertical (TWT) reflection section 8401. They found coincidence of the Moho (velocity step from 6.8 to 8.2 km/s) with the deepest accumulation of consistent near-vertical reflections, and coincidence of the Conrad discontinuity (midcrustal velocity step from 5.4–6.0 to 6.5 km/s) with the upper level of the highly reflective lower crust. An equivalent approach is a depth conversion of the reflection section using the refraction velocity model. Both presume identical horizontal and vertical velocities and are not conclusive in the case of seismic anisotropy. We have preserved the vertical travel-time scale on the reflection sections because of its objective measured character.

A more reliable test for compatibility of reflecting structures in the near-vertical, with first- or second-order velocity discontinuities in the wide-angle range beneath a fixed surface location, is an expanding-spread experiment. In our case the most important crustal discontinuities, the boundary between upper and lower crust and the crust-mantle boundary, are documented continuously from the near-vertical to the wide-angle range in the Haslach region (Sect. 4.2). High-frequency signals and a detector spacing of 80 m enabled a continuous phase correlation and showed coincidence of these discontinuities. This is confirmed by near-vertical and wide-angle modelling presented in Sect. 5.

Another very striking coincidence is observed between the upper-crustal low-velocity zone and a zone of relative transparency in the reflection sections. The base of the low-velocity zone also coincides with the first reflections from the lower crust. Gajewski et al. (1987) determined that the regional extent of the low-velocity zone agrees with the exposed crystalline area of the Black Forest. To the south the low-velocity zone fades out, accompanied by a progressively weaker reflectivity of the lower crust. The coincidence of the low-velocity zone and relatively transparent zone appears to be considered as a special local phenomenon. Otherwise, if correlated with the transparent zone in the EW profile 8403, the low-velocity zone would extend further to the east, as far as the region of the Urach geothermal anomaly (Bartelsen et al., 1982).

The top of the low-velocity zone is neither clearly marked by the reflectivity distribution nor by wide-angle reflections in the expanding-spread profile. It may be of transitional character as well as of undulatory form, following the reflection pattern in the upper crust. Its depth and its interval velocity of 5.4–5.5 km/s are constrained first by the velocity-depth function inferred from the first arrivals, P_G, which show an increase of velocity up to 6 km/s at 6–7 km depth, and second by the average velocity of 5.62 km/s between the surface and the lower crust as inferred from the ESP and the bulk of wide-angle and refraction data.

Strong lateral gravity gradients in the north and south may be related to the "Baden-Baden" and "Badenweiler-Lenzkirch" thrust belts. The gravity minimum in the south coincides with a decrease of reflectivity in the lower crust and the fading out of the low-velocity zone in the upper crust.

Two- and three-dimensional gravity modelling has been performed by Götze et al. (1986). The velocity model of Fig. 32 was transformed to a 2D density model using an empirical velocity-density relationship and inversion techniques. The computed gravity (Fig. 33) fits the observed curve satisfactorily. In the central Black Forest a slight misfit might suggest an additional influence of low-density material in the upper or middle crust. The fading out of the low-velocity/density zone in the south and the subsidence of the lower-crustal isolines is fairly well matched by the computed gravity and the observed data.

In contrast to the velocity-density model, a structure-density model was tested for an accretion hypothesis of underthrusted Paleozoic metasediments, which is supported by structural imaging by the reflection seismics. By optimizing structures and densities, a complete fit could be forced. Gravity modelling may constrain structural models if the results are inconsistent with the data, but consistence is not a general proof of the models. Severe uncertainties may arise from three-dimensional effects of the Rhinegraben which strikes nearly parallel to the gravity survey.

A special phenomenon of interest is the strong Bouguer maximum near the "Baden-Baden" zone in the north,

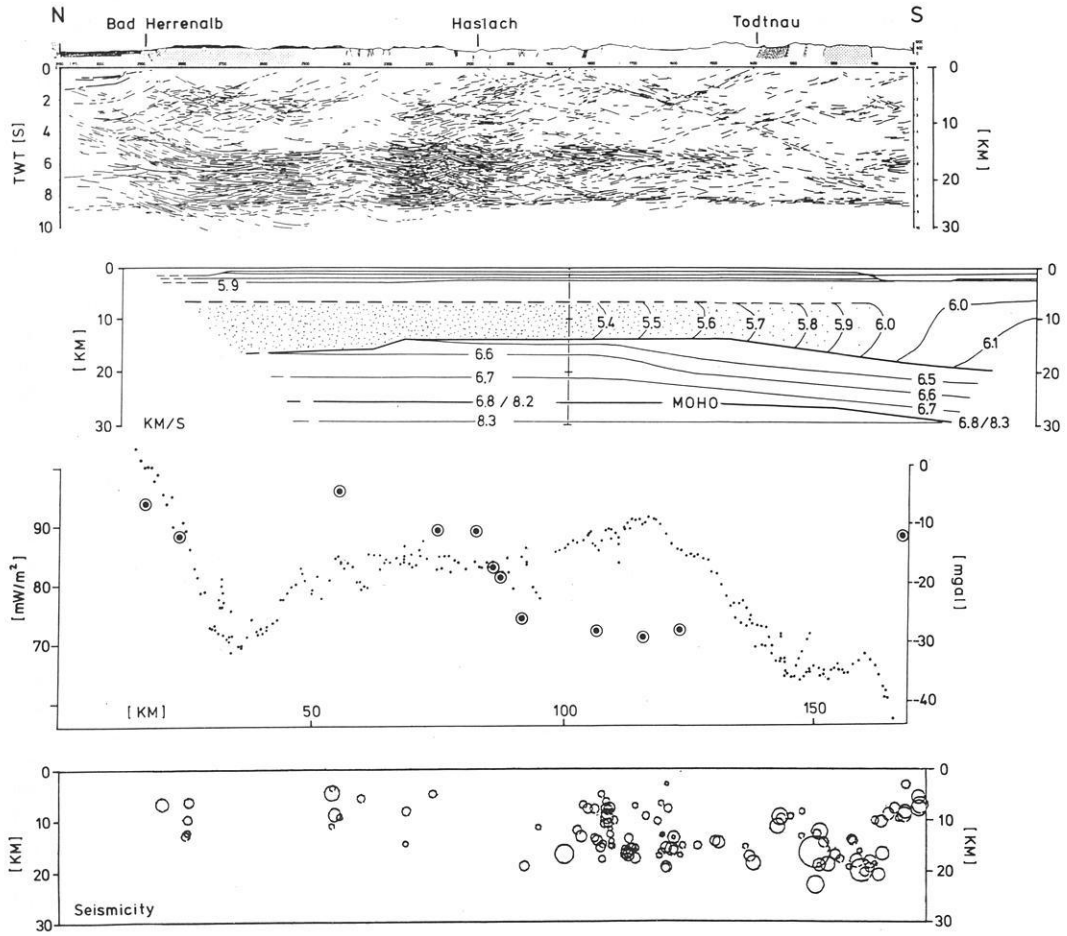

Fig. 32. Compilation of geophysical data for the N–S profile. *From top to bottom:* structural data from the Vibroseis reflection survey (line drawing of migrated line 8401); velocity model from the refraction survey; Bouguer gravity anomaly (*small dots*) and heat flow (*big dots*); seismicity distribution (magnitudes between 1 and 5; projected within a strip of ±10 km width). For references, see text

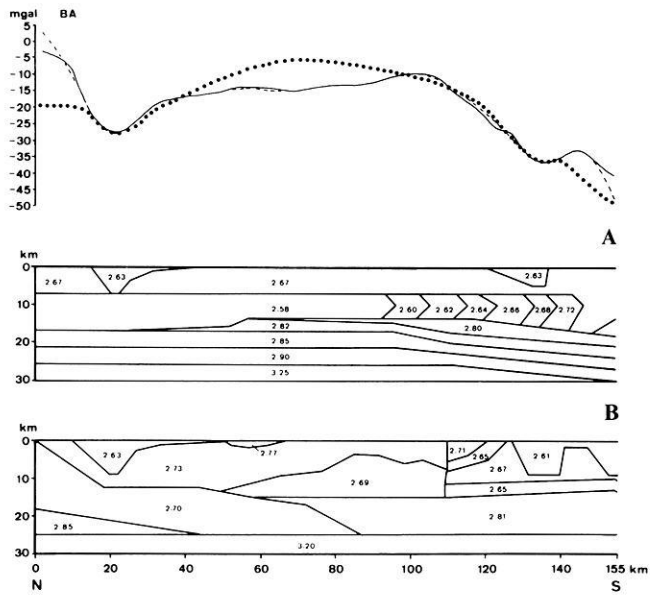

Fig. 33. Gravity modelling. *Upper part:* observed (---) and computed (.... model A, — model B) Bouguer anomaly. *Lower part: A* – velocity model converted to a density model using an empirical relationship. Lower-crustal densities were obtained by an inversion technique. Granite massifs are added for completeness. *B* – structure model based on a hypothetical geological-tectonic model. *Numbers* are densities in g/cm³ (from Götze et al., 1986)

known as the "Kraichgau" anomaly (Fig. 33, left side). The gravity high could be related to a shallow body of mafic-ultramafic material within the Saxothuringian-Moldanubian suture zone. The suture zone is delineated clearly by a strong lateral gravity gradient [cf. gravity map by Gerke (1957)]. Fountain and Salisbury (1981) reported similar gravity anomalies in other continental suture zones. Just north of the Baden-Baden suture zone the reflective character of the lower crust seems to continue into the "Kraichgau" area, revealed by reflections at 5.2 s, 7 s and 9 s (Demnati and Dohr, 1965). This indicates that it originated after the Hercynian suturing, provided that the "lamination" represents the same geological phenomenon both north and south of the Baden-Baden zone. The widespread appearance of the lamination in large areas in Europe suggests non-local geological and physical processes.

Gravity and geomagnetic mapping in the central Black Forest reveal relatively small anomalies with SW–NE trends coincident with the strike of the Hercynian tectonic fabric. Granite bodies such as the "Triberg" granite are clearly displayed by local gravity minima. The maximum depths of the granite bodies are estimated to be about 4-8 km, calculated for granite densities of 2.62 g/cm³ and gneiss densities of 2.73 g/cm³ determined by weighing core samples (Plaumann et al., 1986). This density decrease of 4% corresponds to a velocity decrease of the same amount (cf. Sect. 3.4.1). Reflections from the expected base of the gran-

ite bodies are widely scattered so that corresponding correlations are ambiguous (cf. northern part of profile 8401, locations 2500–2900, Fig. 8). The basal contact between granites and gneisses must be of discontinuous or scattered geometry compared to a seismic wavelength, or it does not represent a contrast of impedance at that depth.

The surface heat flow (Stiefel et al., 1985) is relatively high (70–95 mW/m^2) and shows strong lateral variations. This may be due to increased basal heat flow from the upper mantle, as a consequence of the Rhinegraben rift formation with increased convective and conductive heat transport still active today.

From the rheological point of view, the crust may be subdivided into an upper brittle and a lower ductile part (Chen and Molnar, 1983; Meissner and Strehlau, 1982). The brittle-ductile transition is expected to be represented by the deepest earthquake foci. In the northern part of the cross-section (Fig. 32, lower section), the seismicity is low and maximum hypocentral depth correlates with the reflection-refraction-defined boundary between the upper and lower crust. In the southern part, the seismic activity increases and the foci reach depths of about 20 km. The deepest earthquakes are located within the laminated lower crust.

Magnetotelluric studies revealed a high-conductivity layer (650 S) at midcrustal depths, which cannot, however, be correlated to either the low-velocity zone or to the laminated lower crust, and a pronounced conductivity anisotropy (factor of anisotropy ≥ 5) with maximum conductivity in Hercynian (NE–SW) direction (Berktold et al., 1985; Schmucker and Tezkan, 1987). Recently performed transient electromagnetic soundings in the central Black Forest near Haslach yielded another high-conductivity layer of about 5 Ohm·m dipping to the NW between 9 and 6 km depth (LOTEM Working Group, 1986), correlating with the top of the low-velocity layer.

7.2 Discussion and conclusions

Jones and Nur (1984) and Smithson et al. (1986) have shown by specific field studies, laboratory data of physical properties and seismic modelling that cataclastic fault zones and ductile mylonite zones can be regarded as candidates for upper-crustal reflectors. The seismic structural image of the upper crust in this view is considered as a marker of tectonic events. Figure 34 reflects the basic tectonic interpretation of the seismic sections in the Black Forest. The upper crust is characterized by a rather heterogeneous seismic image. Reflectors are much less continuous than in the lower crust and reveal an increased complexity of structures on a scale of the seismic wavelength (150–300 m). Dominant dipping reflectors seem to die out at a depth of about 8–10 km. In the Black Forest this might be related to a change of the reflective character of a fault zone due to a change of deformation style from a brittle regime with non-cohesive gouge, breccias and random-fabric cataclasites to mylonites. Alternatively, an overprint by recent fluid activity could be taken into account, resulting in a homogenization of seismic structures caused by alterations in mineralogy and petrology. Prominent reflectors in the upper crust in the Black Forest are interpreted in terms of Hercynian tectonic processes. The convergent zones of the Baden-Baden suture zone (BBZ) in the north and the Badenweiler-Lenzkirch zone (BLZ) in the south are visible

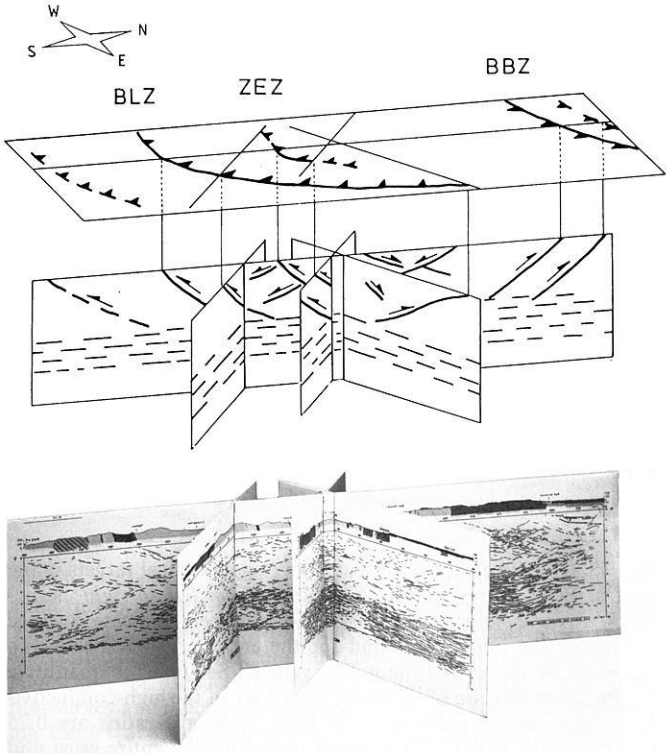

Fig. 34. *Lower part:* Three-dimensional structure diagram provided by line drawings of the net of four reflection profiles. View is from ESE. *Upper part:* Interpretational fence diagram showing Hercynian thrust and late-Hercynian extension tectonics. *BLZ* "Badenweiler-Lenzkirch" zone, *ZEZ* "Zinken-Elme" zone, *BBZ* "Baden-Baden" zone

in the seismic reflection profiles as bands of inclined reflectors. The reflecting band related to the Baden-Baden zone dips 40° to the south and reaches into the deeper crust. On profiles 8401 and 8514, the Badenweiler-Lenzkirch zone can be traced from the surface to a depth of more than 12 km as a number of strongly reflecting elements dipping NW. NW-dipping structures in the eastern section of profiles 8402 and 8403 indicate the continuation of the Badenweiler-Lenzkirch structure beneath the Mesozoic sedimentary cover to the NE. Other NW-dipping reflectors south of the Elztal fault reach a depth of at least 5 km and are interpreted as belonging to another intraplate convergent zone similar to the Badenweiler-Lenzkirch area ("Zinken-Elme" zone, ZEZ). These zones, BBZ, BLZ and ZEZ, constitute thrust faults opposed to each other with northwestward and southeastward vergences (cf. Sect. 2).

Low-angle normal faults characterized by cataclastic deformation in the central Black Forest are identified as reflectors by near-surface high-resolution measurements (Sect. 3.4.2) and are correlated with several SE- and NW-dipping reflectors in this area (see profile 8402). These reflectors, often cross-cutting the reflector pattern, described above, are related to extensional tectonic processes during the late Hercynian and are regarded as markers of the change from compressional to extensional character of the tectonic style.

The lower part of the upper crust (e.g. 7–14 km) is seismically characterized by a *P*-wave low-velocity zone, a reduced V_p/V_s ratio (but no shear-wave velocity inversion) and a zone of relative transparency. This coincides with

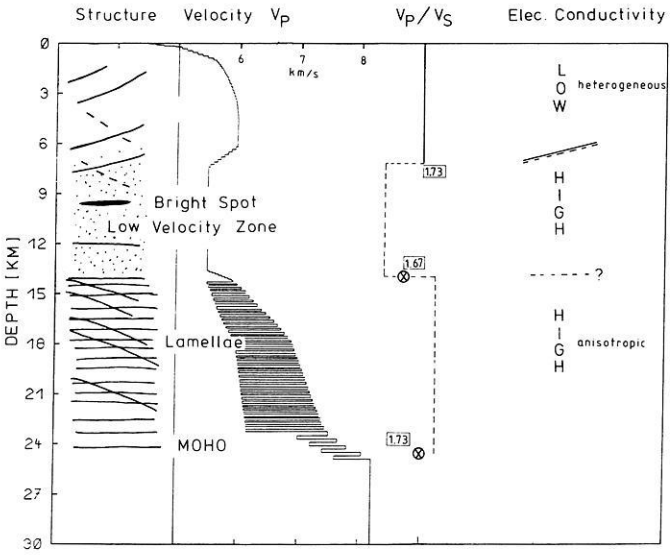

Fig. 35. One-dimensional presentation of geophysical targets in the central Black Forest (Haslach region). *From left to right:* structures, *P*-wave velocities, V_p/V_s ratio (numbers indicate average values for the upper crust and for the entire crust, respectively), electrical conductivity (qualitative values). See text for quantitive values. The precision of the upper boundary of the high-conductivity layer is of the order of 10%–15%. Poisson's ratios are 0.25 ($V_p/V_s = 1.73$), 0.22 (1.67) as mean values for the entire crust and for the upper crust, respectively. The *dashed line* is approximate distribution of local values

a zone of high electrical conductivity (Fig. 35). Model interpretations of the nature of low-velocity zones in re-activated continental crust may include granitic layers (Mueller, 1977), underthrusting of sedimentary rocks and fluid overpressure related to metamorphic or tectonic processes (e.g. Fyfe and Kerrich, 1985). Dehydration reactions during metamorphic processes can reduce the effective pressure at a given crustal level, leading to the formation of new microcracks and thereby lowering the *P*-wave velocity [but increasing the *S*-wave velocity; Kern (1982)]. Velocity inversions can also be triggered by phase transitions in the solid state (quartz) in regions of high heat flow (Kern, 1982).

A bright spot situated in the low-velocity channel is probably caused by a body of lower impedance, which might be taken as evidence for fluid accumulation (Sect. 3.4.3). These completely different observations favour a major role of fluids in a porous or fractured medium, determining physical properties and triggering petrological processes in addition to temperature and pressure. In the Kola deep borehole a low-velocity zone between 4.5 and 9 km depth is characterized by the presence of mineralizing fluids in connection with hydrofracturing, increase in porosity and strong textural variations of the Precambrian rocks (Kremenetsky and Ovchinnikov, 1987). Fuchs et al. (1987) propose a similar mechanism involving dehydration of parts of the lower crust by decompression. The generation of microcracks by fluid overpressure may explain the combined effects of both low-velocity and high electrical conductivity. Also, a layer of decreased velocity and increased conductivity has been found in crystalline rocks of the Urach 3 borehole (Swabian Alb), displaying high microcrack density and strong hydrothermal alteration (Stenger, 1982). The same relationships have been found in the NAGRA borehole, "Böttstein" (NAGRA, 1985).

The lower crust is characterized by a strong and laterally consistent lamination with alternating high and low *P* velocities differing by about 10% and a vertical layering on a scale of 100 m. The horizontal extent of single reflecting elements is in the range of a few hundred metres. The average V_p/V_s ratio in the lower crust is slightly above the crustal mean value of $\sqrt{3}$ (cf. Sect. 4.2). Seismic lamination of the lower crust is a common feature in Hercynian and Caledonian consolidated continental crust (Meissner et al., 1983; Bois et al., 1986; Bortfeld et al., 1985; Matthews and Cheadle, 1986). Lithological interpretations involve compositional or metamorphic layering, underplating, magmatic differentiation, partial melting, fluid enrichment, penetrative ductile deformation (mylonitic banding) or anisotropy.

A great amount of experimental data on velocities of presumed lower-crustal rocks has been published in recent years (Christensen, 1979; Christensen and Fountain, 1975; Fountain, 1976; Kern 1982; Kern and Schenk, 1985; and others). Information on the composition of the lower crust is obtained from outcropping rock series or by analysis of xenoliths in volcanic host rocks. Exposures representing complete lower-crustal sections in Europe (Ivrea zone/western Alps; Calabria/southern Italy) reveal granulite facies rocks, of alternating mafic to acidic composition, as major constituents (Fountain and Salisbury, 1981; Schenk, 1984). Measurements of compressional- and shear-wave velocities in these rocks at lower-crustal PT conditions (Fountain, 1976; Kern and Schenk, 1985) have demonstrated the following relations:

- Both V_p and V_s increase with increasing amount of pyroxene, amphibole, garnet and sillimanite.
- Poisson's ratio is high with high feldspar content and low with high quartz content.
- Strong anisotropy of seismic velocity is caused by preferred lattice orientation of minerals and by metamorphic/compositional layering.
- Metapelitic granulite-facies rocks of intermediate silica and high alumina content have velocities equivalent to mafic granulites ($V_p = 6.8$–7.5 km/s).

Using geophysical and geological data from the Ivrea zone, Hale and Thompson (1982) generated synthetic seismograms with interfering reflections from a stack of thin layers similar to those observed in our reflection data. Blundell and Raynaud (1986) suggested, alternatively, a contribution by sideswipes from a single undulatory surface. Although these lateral effects cannot be completely excluded, a major influence is ruled out by spatial control provided by the intersecting lines.

Anisotropy may be an important factor with respect to the strongly reflecting character of the lower crust. Experimental data on the elastic properties of mylonitic rocks (with anisotropy up to 20%) demonstrate that deep crustal reflections can be explained by extensive ductile deformation of rocks, provided the mylonitic zone is thick enough relative to the seismic wavelength (Jones and Nur, 1984). Late-Hercynian extension of the crust in the Black Forest, which produced cataclastic fault zones in the upper crust, could be accompanied by ductile deformation in the lower crust, thus producing the laminated seismic structure.

Comparative near-vertical and wide-angle observations provide additional hints on the Rhinegraben rift evolution. Fuchs et al. (1987) stressed the identical thickness of about 14 km of the crystalline upper crust beneath both graben

and shoulders, based on near-vertical reflections from the lower crust. They concluded that the upper crust could have subsided about 4 km, without considerable deformation, into the lower crust. Wide-angle observations (Sect. 4.2) indicate a reduced thickness and stronger impedance contrasts of the lamellar structure in the graben proper. These observations favour an origin of the lamellae prior to the beginning of Rhinegraben subsidence and uplift in the Eocene which have modified the pre-existing lamellae. In reflection profiles 8402 and 8514 (see Figs. 10 and 12a), the image of lower-crustal lamination is characterized by more widespread diffraction legs and shorter reflection elements than in profiles 8401 and 8403. This may be due to the presence of line diffractors or elongated lamellae with Hercynian strike perpendicular to profiles 8402 and 8514. This observation is consistent with profiles U1 and U2 of the Urach geothermal project (Bartelsen et al., 1982) and DEKORP 2-South (Bortfeld et al., 1985) and may be regarded as indication of lamellae origin during late Hercynian or Mesozoic extension. Another relationship probably exists to the conductivity anisotropy with preferred Hercynian strike (Berktold et al., 1985). The lower-crustal lamination found by various authors from the BIRPS, ECORS and DEKORP groups, cited above as typical for Hercynian Central and Western Europe, may have its counterpart in the Mesozoic rift margin of the eastern North American coastal plain (Cook et al., 1983).

The crust-mantle boundary has a highly variable appearence in reflection profiles, particularly in those of the COCORP, due to different tectonic regimes, thus reflecting different origins (Oliver, 1982). Its formation might be triggered by thermal events and could represent the final stage of an advanced differentiation process (Meissner and Wever, 1986). Strongly reflecting crust-mantle boundaries often seem to be associated with rifted areas. Klemperer et al. (1986) studied pronounced, mostly horizontally layered Moho reflections in the Basin and Range and found indications favouring an origin by magmatism and extension.

The Moho beneath the Black Forest is developed throughout the entire study area as the deepest horizontally layered and laterally consistent accumulation of high-amplitude reflectors at a relatively shallow depth of 25–27 km. Increasing amplitudes at greater source-receiver offsets indicate that sharp discontinuities or lamallae are superimposed on a velocity-gradient zone of the type determined by Deichmann and Ansorge (1983) for the eastern border of the Black Forest by a refraction survey (Fig. 30). Continuity and truncation relationships with dipping reflectors suggest an age younger than Hercynian. The Moho and horizontal lamellae in the lower crust seem to have overprinted dipping crustal reflectors which delineate thrust zones of Hercynian age (BB zone and BL zone).

The age of the Moho is constrained on one hand by these truncations and by its continuity across suture zones and, on the other hand, by small vertical offsets which are clearly recognized by overlapping diffractions with apices within the Moho, especially in the southeastern part of line 8514 (Fig. 10). If these offsets are markers of tectonic events disrupting a generally rather smooth Moho, they are related to the Alpine orogeny; this favours a Moho age of late-Hercynian to Mesozoic time.

Figure 35 summarizes the relevant geophysical information for the Haslach region. From the structural image of the near-vertical reflection survey, several relics of thrusting and normal faulting can be expected in the upper crust above a very pronounced low-velocity zone coinciding with a relatively transparent zone at 7–8 km depth. A local object of special interest is a bright spot at about 9.5 km depth.

A series of coincident geophysical observations raises crucial geologic-petrological questions concerning recent metamorphic processes and hydrothermal mineralization. The upper-crustal low-velocity zone coincides with a transparent zone where dipping reflectors die out, with a zone of decreased Poisson's ratio (meaning that the *S*-wave velocity is not decreased as much as the *P*-wave velocity) and with a level of high electrical conductivity. These crustal properties seem to be related to recent fluid activity in a porous or fractured medium, to increased basal heat flow and to the brittle-ductile transition. The origin of the geophysical anomalies and gradients is strongly associated with crustal structure, composition and processes.

Acknowledgements. The funding of the KTB reconnaissance program (project RG 8314 6) by the Federal Ministry of Science and Technology, Bonn, is gratefully acknowledged. We thank, especially, H. Schwanitz and his crew from Prakla-Seismos AG, Hannover, for excellent performance during the Vibroseis reflection survey and much helpful cooperation. The DEKORP-Processing Center at Clausthal, directed by R.K. Bortfeld, using hard- and software from Mobil Oil AG, Celle, and Seismograph Service Ltd, London, performed the standard processing. The Geological Survey of Lower Saxony and the DEKORP management, Hannover, A. Hahn, H.-J. Dürbaum, Ch. Reichert and J. Schmoll provided administrative and consultative service. The Thor Geophysikalische Prospektion GmbH, Kiel, provided their pneumatic hammer device and specialists; and the University of Kiel, R. Meissner and H. Stümpel, the recording equipment for the high-resolution surveys. We thank the university teams from the Geophysical Institutes of Zürich, Hamburg, Kiel, Clausthal and Karlsruhe for their enthusiastic participation in the ESP and other experiments. R. Vees (Clausthal) organized pond shot R of the ESP. We are indebted to the entire interdisciplinary Black Forest Working Group for many fruitful and encouraging discussions. In particular, we appreciate the contributions of W. Wimmenauer, K. Schädel, J. Jenkner, B. Jenkner, H. Klein (Freiburg), G. Kleinschmidt, Th. Flöttmann, B. Gallus (Frankfurt), H.-J. Behr (Göttingen), K.-M. Strack (Köln), H-J. Götze, J. Schmalfeldt (Clausthal), A. Stiefel, K.-P. Bonjer, I. Apopei, J. Ebel, D. Gajewski, St. Holbrook, H.-P. Schnell, W. Wälde, P. Blümling, J. Mechie, C. Prodehl (Karlsruhe). A. Stiefel provided the heat-flow data, and K.-P. Bonjer and I. Apopei the seismicity data of Fig. 32. Special thanks are given to D. Gajewski and C. Prodehl for continuous discussions and for their seismic refraction data and results and to K.-M. Strack for the LOTEM contribution.

We appreciate very much the continuous support by the local authorities and individuals, forestry offices, the Baden-Württemberg Mines Office and Geological Survey (Freiburg) and the public media. They all created an animating environment for geoscientific research in the Black Forest. The mayor and the municipal offices of Haslach provided buildings, which served as headquarters for our activities for two years.

We owe our thanks to S.L. Klemperer (BIRPS) for careful and critical reading of the manuscript and for many helpful and stimulating suggestions concerning its content and presentation. We wish to thank G. Müller for his support in editing and publishing this paper.

We thank Mrs. S. Stuhlert for typing the manuscript.

Contribution No. 339 of the Geophysical Institute, Karlsruhe.

Contribution No. 207 of Special Research Program SFB 108 "Stress and Stress Release in the Lithosphere" of Karlsruhe University.

References

Alfred-Wegener-Stiftung: 2nd International Symposium on Observation of the Continental Crust through Drilling (Abstracts) Seeheim, Federal Republic of Germany, Oct. 4–6, 1985, Bonn, 1985

Althaus, E., Behr, H.J., Eder, F.W., Goerlich, F., Maronde, D., Ziegler, W.: Kontinentales Tiefbohrprogramm ("KTB") (Continental Deep Drilling Program) of the Federal Republic of Germany – Advances and status 1984. Terra Cognita **4**, 389–397, 1984

Bartelsen, H., Lüschen, E., Krey, Th., Meissner, R., Schmoll, J., Walther, Ch.: The combined seismic reflection-refraction investigation of the Urach Geothermal anomaly. In: The Urach geothermal project, R. Haenel, ed.: pp. 247–262. Schweizerbart'sche Verlagsbuchhandlung, Stuttgart 1982

Behr, H.-J., Engel, W., Franke, W., Giese, P., Weber, K.: The Variscan belt in Central Europe: main structures, geodynamic implications, open questions. In: H.J. Zwart, H.-J. Behr and J. Oliver (eds.), Appalachian and Hercynian Fold Belts. Tectonophysics **109**, 15–40, 1984

Berktold, A., Musmann, G., Tezkan, B., Wohlenberg, J.: Electrical conductivity studies, Schwarzwald Working Group. Abstract, 2nd International Symposium on Observation of the Continental Crust through Drilling, Alfred-Wegener-Stiftung, Bonn, October 4–6, 1985, p. 70, 1985

Blackburn, G.: Errors in stacking velocity – true velocity conversion over complex geologic situations. Geophysics **45**, 1465–1488, 1980

Blundell, D.J., Raynaud, B.: Modeling lower crust reflections observed on BIRPS profiles. In: Reflection seismology: a global perspective, M. Barazangi, L. Brown, eds.: pp. 287–295. Geodynamics Series Volume 13, American Geophysical Union, Washington, D.C. 1986

Bois, C., Cazes, M., Damotte, B., Galdéano, A., Hirn, A., Mascle, A., Matte, P., Raoult, J.F., Torreilles, G.: Deep seismic profiling of the crust in northern France: the ECORS project. In: Reflection seismology: a global perspective, M. Barazangi, L. Brown, eds.: pp. 21–29. Geodynamics Series Volume 13, American Geophysical Union, Washington, D.C. 1986

Bonjer, K.-P., Apopei, I., Lüschen, E., Fuchs, K., Sandmeier, K.-J.: The Glottertal – 1986 micro-earthquake sequence – evidence of brittle deformation in the upper crustal reflector. Abstract of Poster Program, 2. KTB Kolloquium 19.9–21.9.1986 Seeheim, p. 54, 1986

Bortfeld, R.K., Gowin, J., Stiller, M., Baier, B., Behr, H.J., Heinrichs, T., Dürbaum, H.J., Hahn, A., Reichert, C., Schmoll, J., Dohr, G., Meissner, R., Bittner, R., Milkereit, B., Gebrande, H.: First results and preliminary interpretation of deep-reflection seismic recordings along profile DEKORP 2-South. J. Geophys. **57**, 137–163, 1985

Brown, L., Barazangi, M., Kaufman, S., Oliver, J.: The first decade of COCORP: 1974–1984. In: Reflection seismology: a global perspective, M. Barazangi, L. Brown, eds.: pp. 107–120. Geodynamics Series Volume 13, American Geophysical Union, Washington, D.C. 1986

Censor, Y: Finite series-expansion reconstruction methods. Proc. IEEE **71**, 409–419, 1983

Chen, W.-P., Molnar, P.: Focal depths of intercontinental and intraplate earthquakes and their implications for the thermal and mechanical properties of the lithosphere. J. Geophys. Res. **88**, 4183–4214, 1983

Christensen, N.I.: Compressional wave velocities in rocks at high temperatures and pressures. Critical thermal gradients, and crustal low-velocity zones. J. Geophys. Res. **84**, 6849–6857, 1979

Christensen, N.I., Fountain, D.M.: Constitution of the lower crust based on experimental studies of seismic velocities in granulite. Geol. Soc. Amer. Bull. **86**, 227–236, 1975

Cook, F.A., Brown, L.D., Kaufman, S., Oliver, J.E.: The COCORP seismic reflection traverse across the southern Appalachians. American Association of Petroleum Geologists Studies in Geology **14**, 61 p., 1983

Damotte, B., Fuchs, K., Lüschen, E., Wenzel, F., Schlich, R., Torreilles, G.: Wide angle Vibroseis test across the Rhinegraben. Geophys. J.R. Astron. Soc. **89**, 313–318, 1987

Deichmann, N., Ansorge, J.: Evidence for lamination in the lower continental crust beneath the Black Forest (southwestern Germany). J. Geophys. **52**, 109–118, 1983

Demnati, A., Dohr, G.: Reflexionsseismische Tiefensondierungen im Bereich des Oberrheingrabens und des Kraichgaues. Z. Geophys. **31**, 229–245, 1965

De Vries, D., Berkhout, A.J.: Influence of velocity errors on the focusing aspects of migration. Geophys. Prospecting **32**, 629–648, 1984

Dinstel, W.L.: Velocity spectra and diffraction patterns. Geophysics **36**, 415–417, 1971

Dix, C.H.: Seismic velocities from surface measurements. Geophysics **20**, 68–86, 1955

Dohr, G.: Reflexionsseismische Messungen im Oberrheingraben mit digitaler Aufzeichnungstechnik und Bearbeitung. In: Graben problems, J.H. Illies, S. Mueller, eds.: pp. 207–218. Schweizerbart'sche Verlagsbuchhandlung, Stuttgart 1970

Edel, J.B., Fuchs, K., Gelbke, C., Prodehl, C.: Deep structure of the southern Rhinegraben area from seismic refraction investigations. J. Geophys. **41**, 333–356, 1975

Emmermann, R.: A petrogenetic model for the origin and evolution of the Hercynian granite series of the Schwarzwald. Neues Jahrb. Mineral. Abh. **128**, 219–253, 1977

Finckh, P., Frei, W., Fuller, B., Johnson, R., Mueller, St., Smithson, S., Sprecher, Chr.: Detailed crustal structure from a seismic reflection survey in northern Switzerland. In: Reflection seismology: a global perspective, M. Barazangi, L. Brown, eds.: pp. 43–54. Geodynamics Series Volume 13, American Geophysical Union, Washington, D.C. 1986

Fountain, D.M.: The Ivrea-Verbano and Strona-Ceneri zones, northern Italy: a cross-section of the continental crust – New evidence from seismic velocities of rock samples. Tectonophysics **33**, 145–165, 1976

Fountain, D.M., Salisbury, M.H.: Exposed cross-sections through the continental crust: implications for crustal structure, petrology, and evolution. Earth Planet. Sci. Letts. **56**, 263–277, 1981

Fromm, G.: Ermittlung statischer Grundkorrekturen. In: Erfassung seismischer Daten, 4. Mintrop-Seminar 1984, L. Dresen, J. Fertig, H. Rüter, W. Budach, eds.: pp. 253–313, 1984

Fuchs, K.: On the properties of deep crustal reflectors. Z. Geophys **35**, 133–149, 1969

Fuchs, K., Mueller, G.: Computation of synthetic seismograms with the reflectivity method and comparison with observations. Geophys. J.R. Astron. Soc. **23**, 417–423, 1971

Fuchs, K., Bonjer, K.-P., Gajewski, D., Lüschen, E., Prodehl, C., Sandmeier, K.-J., Wenzel, F., Wilhelm, H.: Crustal evolution of the Rhinegraben area. I. Exploring the lower crust in the Rhinegraben rift by unified geophysical experiments. Tectonophysics, in press, 1987

Fyfe, W.S., Kerrich, R.: Fluids and thrusting. Chem. Geol. **49**, 353–362, 1985

Gajewski, D., Prodehl, C.: Seismic refraction investigation of the Black Forest. Tectonophysics, in press, 1987

Gajewski, D., Holbrook, W.S., Prodehl, C.: Three-dimensional crustal structure of southwest Germany, derived from seismic-refraction data. Tectonophysics, in press, 1987

Gazdag, J.: Modeling of the acoustic wave equation with transform methods. Geophysics **46**, 854–859, 1981

Gebrande, H.: CMP-Refraktionsseismik. In: Seismik auf neuen Wegen, 6. Mintrop-Seminar 1986, L. Dresen, J. Fertig, H. Rüter, W. Budach, eds.: pp. 191–205, 1986

Gerke, K.: Die Karte der Bouguer-Isanomalien 1:1.000.000 von Westdeutschland. Frankfurt/Main: Institut für Angewandte Geodäsie 1957

Giese, P.: Depth calculation. In: Explosion seismology in Central Europe, P. Giese, C. Prodehl, A. Stein, eds.: pp. 146–161, 1976

Gordon, R., Bender, R., Herman, G.T.: Algebraic reconstruction techniques (ART) for three-dimensional electron microscopy and x-Ray photography. J. Theor. Biol. **29**, 471–481, 1970

Götze, H.-J., Schmalfeldt, J., Wagener, M.: Gravimetrische und magnetische Vorerkundung im Schwarzwald. Internal KTB communication, reported in: Kontinentales Tiefbohrprogramm der Bundesrepublik Deutschland KTB, Ergebnisse der Vorerkundungsarbeiten Lokation Schwarzwald, v. Gehlen et al., eds.: pp. 29–30. 2. KTB-Kolloquium Seeheim/Odenwald, 19.9.–21.9.1986, 1986

Hacker, W., Hirschmann, G.: Ältere und jüngere Thrust-Tektonik im Zentralschwarzwälder Gneiskomplex. Internal KTB communication, reported in: Kontinentales Tiefbohrprogramm der Bundesrepublik Deutschland KTB, Ergebnisse der Vorerkundungsarbeiten Lokation Schwarzwald, v. Gehlen et al., eds.: p. 76ff. 2. KTB-Kolloquium Seeheim/Odenwald, 19.9.–21.9. 1986, 1986

Hagedoorn, J.G.: The plus-minus method of interpreting seismic refraction sections. Geophys. Prospecting **7**, 158–182, 1959

Hajnal, Z., Sereda, I.T.: Maximum uncertainty of interval velocity estimates. Geophysics **46**, 1543–1547, 1981

Hale, L.D., Thompson, G.A.: The seismic reflection character of the continental Mohorovicic discontinuity. J. Geophys. Res. **87**, 4625–4635, 1982

Illies, J.H.: Mechanism of graben formation. Tectonophysics **73**, 249–266, 1981

Illies, J.H., Fuchs, K. (eds.): Approaches to taphrogenesis. Stuttgart: Schweizerbart'sche Verlagsbuchhandlung 1974

Illies, J.H., Mueller, S. (eds.): Graben problems. Stuttgart: Schweizerbart'sche Verlagsbuchhandlung 1970

Jones, T.D., Nur, A.: The nature of seismic reflections from deep crustal fault zones. J. Geophys. Res. **89**, 3153–3171, 1984

Kern, H.: P- and S-wave velocities in crustal and mantle rocks under the simultaneous action of high confining pressure and high temperature and the effect of the rock microstructure. In: High-pressure researches in geoscience, W. Schreyer, ed.: pp. 15–45. Schweizerbart'sche Verlagsbuchhandlung, Stuttgart 1982

Kern, H., Schenk, V.: Elastic wave velocities in rocks from a lower crustal section in southern Calabria (Italy). Phys. Earth Planet. Inter. **40**, 147–160, 1985

Ketelsen, K., Marschall, R., Fromm, G.: Automatic picking of first arrivals with two-sided signals (Vibroseis). 45th E.A.E.G. Meeting, Oslo, Norway 1983

Klein, H., Wimmenauer, W.: Eclogites and their retrograde transformation in the Schwarzwald. Neues Jahrb. Mineral. Monatsh. 25–38, 1984

Klemperer, S.L., Hauge, T.A., Hauser, E.C., Oliver, J.E., Potter, C.J.: The Moho in the northern Basin and Range province, Nevada, along the COCORP 40° N seismic-reflection transect. Geol. Soc. Amer. Bull. **97**, 603–618, 1986

Kosloff, D.D., Baysal, E.: Forward modeling by a Fourier method. Geophysics **47**, 1402–1412, 1982

Kremenetsky, A.A., Ovchinnikov, L.N.: The Precambrian continental crust: its structure, composition and evolution as revealed by deep drilling in the U.S.S.R. Precambrian Res. **33**, 11–43, 1987

Lerwill, W.E.: The amplitude and phase response of a seismic vibrator. Geophys. Prospecting **29**, 503–528, 1981

Lippolt, H.J., Schleicher, H., Raczek, I.: Rb–Sr systematics of Permian volcanics in the Schwarzwald (SW Germany). Contrib. Mineral. Petrol. **84**, 272–280, 1983

Lorenz, V., Nicholls, I.A.: Plate and intraplate processes of Hercynian Europe during the Late Paleozoic. Tectonophysics **107**, 25–56, 1984

LOTEM Working Group: Schwarzwald, LOTEM-Tiefensondierung. Abstract of Poster Program, 2. KTB-Kolloquium, 19.9.–21.9.1986, Seeheim, p. 48, 1986

Matte, Ph.: Tectonics and plate tectonics model for the Variscan belt of Europe. Tectonophysics **126**, 329–374, 1986

Matthews, D.H., Cheadle, M.J.: Deep reflections from the Caledonides and Variscides west of Britain and comparison with the Himalayas. In: Reflection seismology: a global perspective, M. Barazangi, L. Brown, eds.: pp. 5–19. Geodynamics Series Volume 13, American Geophysical Union, Washington, D.C. 1986

Meissner, R., Strehlau, J.: Limits of stresses in continental crusts and their relation to the depth-frequency distribution of shallow earthquakes. Tectonics **1**, 73–89, 1982

Meissner, R., Wever, Th.: Nature and development of the crust according to deep reflection data from the German Variscides. In: Reflection seismology: a global perspective, M. Barazangi, L. Brown, eds.: pp. 31–42. Geodynamics Series Volume 13, American Geophysical Union, Washington, D.C. 1986

Meissner, R., Lüschen, E., Flüh, E.R.: Studies of the continental crust by near-vertical reflection methods: a review. Phys. Earth Planet. Inter. **31**, 363–376, 1983

Miller, M.K.: Stacking of reflections from complex structures. Geophysics **39**, 427–440, 1974

Morton, J.L., Sleep, N.H.: Seismic reflections from a Lau Basin magma chamber. In: Geology and offshore resources of Pacific island arcs – Tonga region, D.W. Scholl, T.L. Vallier, eds.: pp. 441–453. Circum-Pacific Council for Energy and Mineral Resources Earth Science Series, vol. 2, Houston, 1985

Mueller, St.: A new model of the continental crust. In: The Earth's crust, J.G. Heacock, ed.: pp. 289–317. Geophys. Monogr. Series **20**, American Geophysical Union, Washington, D.C. 1977

Mueller, St., Peterschmitt, E., Fuchs, K., Ansorge, J.: Crustal structure beneath the Rhinegraben from seismic refraction and reflection measurements. Tectonophysics **8**, 529–542, 1969

NAGRA: Technischer Bericht 85-01, Textband und Beilagenbände A und B. Nationale Genossenschaft für die Lagerung radioaktiver Abfälle, Baden, 1985

Oliver, J.E.: Changes at the crust-mantle boundary. Nature **299**, 398–399, 1982

Peddy, C., Brown, L.D., Klemperer, S.L.: Interpreting the deep structure of rifts with synthetic seismic sections. In: Reflection seismology: a global perspective, M. Barazangi, L. Brown, eds.: pp. 301–311. Geodynamics Series Volume 13, American Geophysical Union, Washington, D.C. 1986

Plaumann, S., Groschopf, R., Schädel, K.: Kompilation einer Schwerekarte und einer geologischen Karte für den mittleren und nördlichen Schwarzwald mit einer Interpretation gravimetrischer Detailvermessungen. Geol. Jahrb. **E 33**, 15–30, 1986

Prodehl, C., Ansorge, J., Edel, J.B., Emter, D., Fuchs, K., Mueller, S., Peterschmitt, E.: Explosion seismology research in the central and southern Rhine Graben – a case history. In: Explosion seismology in Central Europe. P. Giese, C. Prodehl, A. Stein, eds.: pp. 313–328. Berlin: Springer Verlag 1976

Rühl, Th.: Tauchwellen-Tomographie für Stripping-Korrekturen und geologische Interpretationen bei den reflexionsseismischen KTB-Profilen im Schwarzwald. Diploma Thesis, Geophysical Institute of the University of Karlsruhe, 1987

Sandmeier, K.-J., Wenzel, F.: Synthetic seismograms for a complex crustal model. Geophys. Res. Lett. **13**, 22–25, 1986

Schenk, V.: Petrology of felsic granulites, metapelites, metabasics, ultramafics, and metacarbonates from Southern Calabria (Italy): prograde metamorphism, uplift and cooling of a former lower crust. J. Petrol. **25**, 255–298, 1984

Schmucker, U., Tezkan, B.: Zur Deutung regional einheitlicher Richtungsabhängigkeiten tellurischer Variationen. 47th Ann. Meeting of Dtsch. Geophys. Gesell., Clausthal-Zellerfeld, 31.3.–4.4.1987

Schnell, H.P.: Untersuchung des Einflusses oberflächennaher Schichten auf seismische Signale und Beiträge zur Optimierung des Vibroseis-Verfahrens. Diploma Thesis, Geophysical Institute of the University of Karlsruhe, 1987

Sheriff, R.E., Geldart, L.P.: Exploration seismology, Volume 2. Data-processing and interpretation. Cambridge: Cambridge University Press, 1983

Sittig, E.: Zur geologischen Charakterisierung des Moldanubikums

am Oberrhein (Schwarzwald). Oberrh. Geol. Abh. **18**, 119–161, 1969

Slichter, L.B.: The theory of the interpretation of seismic travel time curves in horizontal structures. Physics **3**, 273–295, 1932

Smithson, S.B., Johnson, R.A., Hurich, C.A.: Crustal reflections and crustal structure. In: Reflection seismology: the continental crust, M. Barazangi, L. Brown, eds.: pp. 21–32. Geodynamics Series Volume 14, American Geophysical Union, Washington, D.C. 1986

Stenger, R.: Petrology and geochemistry of the basement rocks of the Research Drilling Project Urach 3. In: The Urach Geothermal Project, R. Haenel, ed.: pp. 41–47. Schweizerbart'sche Verlagsbuchhandlung, Stuttgart 1982

Stiefel, A., Wilhelm, H., Finkbeiner, K., Haack, U.: Geothermal studies, Schwarzwald. Abstract of poster, 2nd International Symposium on Observation of the Continental Crust through Drilling, Alfred-Wegener-Stiftung, October 4–6, 1985, Seeheim, p. 72, 1985

Vogelsang, D.: Geothermische und geologische Vorerkundung der Tiefbohrlokation Oberpfalz und Schwarzwald. Teilgebiet Bohrlochgeophysik Schwarzwald. Bericht NLfB Hannover, Archiv-Nr. 99126, 1986

Warner, M.: Migration – why doesn't it work for deep continental data? Geophys. J.R. Astron. Soc. **89**, 21–26, 1987

Walther, Ch., Trappe, H., Meissner, R.: The detailed velocity structure of the Urach geothermal anomaly. J. Geophys. **59**, 1–10, 1986

Wenzel, F., Sandmeier, K.-J., Wälde, W.: Properties of the lower crust from modeling refraction and reflection data. J. Geophys. Res., in press, 1987

Wimmenauer, W., Adam, A.: High-pressure phenomena in acid rocks accompanying eclogites in the Schwarzwald (SW Germany). Terra Cognita **5**, 426, 1985

Winterstein, D.F.: Anisotropy effects in P-wave and SH-wave stacking velocities contain information on lithology. Geophysics **51**, 661–672, 1986

Zucca, J.J.: The crustal structure of the southern Rhinegraben from re-interpretation of seismic refraction data. J. Geophys. **55**, 13–22, 1984

Received January 27, 1987; revised June 16, 1987
Accepted June 17, 1987